

Graduate School of Engineering, Nagasaki University

**Development of Automated Water Quality Monitoring
Techniques for Producing Safe Drinking Water**

A thesis submitted in partial fulfillment
of the requirements for the degree of

Doctor of Philosophy

From

Nagasaki University

By

BOIVIN Sandrine Lucie Pascale

December 2021

[This page intentionally left blank]

Abstract

From the water source to the produced drinking water, water treatment plants have developed different treatment trains to deliver quality drinking water. However, many challenges remain. We developed three monitoring techniques. First, a facile method for counting odor-producing algae (*Pseudanabaena* sp.) in water source was designed to enhance the quality of drinking water. Then to improve microbial safety, the reliability of a real-time bacteriological counter coupled with an online dialysis membrane-based pre-treatment system was evaluated. Lastly, we developed a nanofiltration membrane-based pre-treatment system for continuously analyzing the concentrations of bromate ions in treated wastewater.

For many drinking water utilities, predicting odor occurrence in drinking water sources is a major challenge. *Pseudanabaena* sp. was found to be responsible for odor peak at low level concentration in lake water. It can be used as a surrogate indicator for 2-methylisoborneol (2-MIB) concentration in lake water. The fluorescence emitted by chlorophyll was relatively weak and uniform throughout the cells for cyanobacteria like *Pseudanabaena* sp., whereas other algae such as diatoms and green algae showed highly variable auto-fluorescence intensity in their cells. This difference of fluorescence intensity allowed us to discriminate cyanobacteria from all other algae. Among cyanobacteria, the length and width of *Pseudanabaena* sp. were unique; thus, dimensions and fluorescence intensity were the criteria selected to recognize only *Pseudanabaena* sp. among algae. The developed auto-counting method was successfully validated. Manually and automatically counted *Pseudanabaena* sp. in lake water samples were highly correlated. Although the developed method can overestimate *Pseudanabaena* sp. counts due to the presence of other similar-sized algae, this facile method permits frequent on-site analysis by water treatment plant workers without analytical skills. Providing early warnings of potential 2-MIB occurrence enables the drinking water treatment plants to take suitable precautionary countermeasures.

Real-time bacteriological counting technology is capable of providing an online profile of bacterial removal during the water treatment process, and can enhance the safety of water. However, dissolved organic compounds present in treated wastewater and freshwaters have strong autofluorescence, interfering with the analysis by masking the weak autofluorescence emitted from bacteria. The reliability of real-time bacteriological counter coupled with an online dialysis membrane-based pre-treatment system was evaluated for continuous monitoring bacterial counts in sand filter effluents of a full-scale drinking water

treatment plant. The pre-treatment system, which included anion exchange resins for dialysate regeneration, successfully achieved the stable attenuation of background interfering substances (humic acids) during 19 days. The real-time bacteriological counter equipped with the pre-treatment system provided a continuous profile of bacterial counts in the sand filter effluent ($0.2\text{--}2.5\times 10^4$ counts/mL). The online analysis identified different timing of concentration peaks between particle and bacterial counts after backwashing. Further, total bacterial counts determined by fluorescence microscopy and SYBR[®] Green I staining, a commonly accepted parameter, was found to be an indicator of online-monitored bacterial counts. Bacterial community analysis revealed that Proteobacteria, Planctomycetes, and Cyanobacteria were the dominating phyla, which was the same as expected according to previous studies. The results indicated the potential of the real-time bacteriological counter for providing an early warning of filter failures, which can allow plant operators to diagnose the overall system and provide countermeasures.

Continuous monitoring of bromate ions, a disinfection by-product of the ozonation of wastewater, may improve the safety of recycled water for potable use. A recently developed elemental analyzer can determine bromate ion concentrations online. However, dissolved organics present in wastewater interfere with the detection of bromate ions. The aim of this study was to develop a nanofiltration (NF) membrane-based pre-treatment system to remove the interfering substances present in treated wastewater prior to the online analysis. The NF pre-treatment system was optimized to ensure the removal of the interfering substances from the membrane bioreactor (MBR)-treated wastewater without altering the bromate ion concentration. We determined a permeate flux of $1\text{ L/m}^2\text{ h}$ and a feed temperature of $35\text{ }^\circ\text{C}$ as optimal pre-treatment conditions for online analysis. Furthermore, the continuous monitoring of MBR-treated wastewater, containing different bromate ion concentrations ($0\text{--}12\text{ }\mu\text{g/L}$), for three days revealed a strong correlation between the concentrations determined using the online analyzer and liquid chromatography coupled with tandem mass spectrometry. Thus, this study demonstrates the potential utility of the online bromate ion analyzer coupled with NF pre-treatment system to monitor the rate of bromate ion formation during ozonation.

Acknowledgements

I would like to express my sincere gratitude for the opportunity to work on this PhD. I would like to give special thanks to Professor Shuji Tanabe for providing support and feedback throughout this project. I would like to express the deepest appreciation to Associate Professor Takahiro Fujioka for his guidance. Without his invaluable help, dedicated support and overall insights, this achievement on my PhD work would not have been possible.

I would like to thank METAWATER and the Sasebo City Waterworks Bureau for helping with in samples collection, sharing various related data and providing support with algal identification. I also thank Azbil Corporation and METAWATER for lending their equipment.

My thanks and appreciations also go to my colleagues in the same laboratory who have willingly helped me out with their abilities. Finally, I cannot forget to thank my father and my family for their unconditional support, help and patience. My husband and children have been a great source of motivation.

List of publications

Major publications

- (1) BOIVIN Sandrine, HASEGAWA Eri, YAMAGUCHI Davide, FUJIOKA Takahiro; A Facile Technique for Automatically Counting Odor-producing Algae (*Pseudanabaena* sp.) in Drinking Water Sources, *Environmental Science: Water Research & Technology*, 7, pp. 1032–1039 (2021.4) (Chapter 4).
- (2) FUJIOKA Takahiro, BOIVIN Sandrine, TAKEUCHI Haruka; Online Monitoring of Bromate in Treated Wastewater: Implications for Potable Water Reuse, *Environmental Science: Water Research & Technology*, In press (Accepted, 2021.10) (Chapter 7).
- (3) BOIVIN Sandrine, TANABE Shuji, FUJIOKA Takahiro; Online evaluation of bacterial particles in sand filter effluents of a full-scale drinking water treatment plant, *Science of the Total Environment*, Submitted on 15 October 2021 (Chapter 6).

Other publications

- (1) NGO Thi Tra My, Diep Binh Quoc, SANO Hideaki, NISHIMURA Yasuhiro, BOIVIN Sandrine, KODAMATANI Hitoshi, TAKEUCHI Haruka, SAKTI Satya Candra Wibawa, FUJIOKA Takahiro; Membrane distillation for achieving high water recovery for potable water reuse, In press (Accepted on 18 October 2021).
- (2) BOIVIN Sandrine, TRAN Hai Minh Duc, KODAMATANI Hitoshi, IKEHATA Keisuke, FUJIOKA Takahiro, Potential of UV-B and UV-C irradiation in disinfecting microorganisms and removing *N*-nitrosodimethylamine and 1,4-dioxane for potable water reuse: A review, *Chemosphere*, 286 (2), 131682, pp. 131682 (2022. 1).
- (3) FUJIOKA Takahiro, NGO My Thi Tra, MAKABE Ryo., BOIVIN Sandrine, IKEHATA Keisuke; Pre-treatment of Surface Waters and Wastewater by a Hemodiafilter for Online Bacterial Counting, *Environmental Science & Technology Water*, 1 (1), pp. 101–107 (2021. 1).
- (4) FUJIOKA Takahiro, NGO My Thi Tra, MOCHOKO Tanki, BOIVIN Sandrine, OHKUMA Naoki, YASUI Hidenari, TERASHIMA Mitsuharu; Biofouling Control of a Forward Osmosis Membrane during Single-pass Pre-concentration of Wastewater, *Chemosphere*, 257, pp. 127263 (2020. 10).

- (5) FUJIOKA Takahiro and BOIVIN Sandrine; Assessing Bacterial Infiltration through Reverse Osmosis Membrane, *Environmental Technology & Innovation*, 19, pp. 100818 (2020. 8).
- (6) FUJIOKA Takahiro, NGO My Thi, Tra, BOIVIN Sandrine, KAWAHARA Kengo, TAKADA Akihiro, NAKAMUR Yuki, YOSHIKAWA Hiro; Controlling Biofouling and Disinfection By-product Formation during Reverse Osmosis Treatment for Seawater Desalination, *Desalination*, 488, pp. 114507 (2020. 8).
- (7) FUJIOKA Takahiro and BOIVIN Sandrine; Dialysis as a New Pre-treatment Technique for Online Bacterial Counting, *Science of the Total Environment*, 714, 136768 (2020. 4)
- (8) FUJIOKA Takahiro, YOSHIKAWA Hiro, EGUCHI Masahiro, BOIVIN Sandrine, KODAMATANI Hitoshi; Application of Stabilized Hypobromite for Controlling Membrane Fouling and N-nitrosodimethylamine Formation, *Chemosphere*, 240, pp. 124939 (2020. 2).
- (9) FUJIOKA Takahiro and BOIVIN Sandrine; Assessing the Passage of Particles through Polyamide Reverse Osmosis Membranes, *Separation and Purification Technology*, 226, pp. 8-12 (2019. 1).

Conference Presentations

- (1) Boivin, S., Hasegawa, E., Yamaguchi, D., Fujioka, T.; A facile technique for automatically counting odor-producing algae (*Pseudanabaena* sp.) in drinking water sources, the 2020 Japan Society on Water Environment Kyushu-Okinawa Branch Conference (Sai-Yuusyusyou, Mizukankyō Gakkai Kyushu-Okinawa Shibu Kenkyū Hapyou Kai), 16th March 2021 (Online)

*BOIVIN Sandrine, First-place Award for Excellence

[This page intentionally left blank]

Table of Contents

Chapter 1	Introduction.....	1
1.1.	Background	1
1.2.	Research objectives	2
1.3.	Thesis outlines.....	2
Chapter 2	Literature review	3
2.1.	Odor occurrence in drinking water sources.....	3
2.2.	Bacterial monitoring during sand filtration.....	6
2.3.	Online monitoring of bromate.....	8
Chapter 3	Materials and methods	11
3.1.	Algal counting	11
3.1.1.	Water samples.....	11
3.1.2.	Odor quantification	13
3.1.3.	Microscope and sample preparation	13
3.1.4.	Bright-field observation	14
3.1.5.	Fluorescence observation.....	14
3.1.6.	Auto-counting method development and validation.....	15
3.2.	Online bacterial counting	16
3.2.1.	The sand filtration process	16
3.2.2.	Dialysis membrane-based pre-treatment system	17
3.2.3.	Real-time bacteriological counter	18
3.2.4.	Manual bacterial counts	19
3.2.5.	Bacterial community analysis	21
3.2.6.	Excitation emission matrix spectrum.....	21
3.3.	Online monitoring of bromate.....	21
3.3.1.	Materials	21
3.3.2.	Analytical methods	22
3.3.3.	The NF pretreatment system.....	24
3.3.4.	Experimental protocols	25
Chapter 4	Algal counting.....	27
4.1.	Identification of an odor-producing algae.....	27

4.2.	Automated counting technique development	31
4.3.	Fluorescence observations.....	31
4.4.	Validation of the developed method	37
4.5.	Practical applications.....	43
Chapter 5	Online monitoring of bacteria.....	45
5.1.	Online bacterial counts and pre-treatment performance	45
5.1.1.	Bacterial counts in the rapid sand filter effluent.....	45
5.1.2.	The fate of bacteria before and after backwashing	48
5.1.3.	Stability of pre-treatment	50
5.2.	Bacteria in the rapid sand filter effluent.....	55
5.2.1.	Assessment of bacterial community	55
5.2.2.	Assessment of the bacterial quantity.....	60
Chapter 6	Online monitoring of bromate	65
6.1.	Importance of the NF pre-treatment system.....	65
6.2.	Optimization of pre-treatment conditions	67
6.3.	Validations in the online analysis results	71
6.4.	Implications for on-site use	74
Chapter 7	Conclusions.....	75
Chapter 8	Future research	77
References		78

Chapter 1 Introduction

1.1. Background

For drinking water two main factors are critically important: the quality and the safety. Although not a public health threat, odor in drinking water is a major challenge faced by many water utilities as bad odor leads to complaints from consumers (Watson, 2004; Winter et al., 2011). Odor in water is often due to the presence of 2-methylisoborneol (2-MIB) and/or geosmin, which are typically produced by specific algae. According to climate change and eutrophication of lakes, algal blooms associated with odor have occurred more frequently and lasted longer in recent years. The water treatment plants generally add powdered activated carbon (PAC) to remove the odor. However, PAC cannot be promptly added due to lack of techniques for assessing the odor concentration swiftly. For example, 2-MIB analysis at regulated levels in Japan (10 ng/L) requires sample pretreatment, skilled analysts, and a GC-MS/MS; thus, often this analysis is conducted infrequently (e.g., once a week). As a result, a sudden change in the odor levels in source water results in periods of non-compliance with odor regulations.

About the safety of drinking water, a particular focus is placed on the microbial load. Water authorities in many countries are regulated to periodically evaluate microbiological safety by analyzing culturable indicator bacteria such as *Escherichia coli*. However most of the bacteria in drinking water are not culturable. Even if online instruments measuring surrogate indicators (turbidity and particle counts) are typically used to provide a warning of a potential contamination, the implementation of microbiological sensors or rapid detection methods that can continuously provide the concentration of microorganisms can enhance the safety of drinking water (Lee and Deininger, 1999; Van Nevel et al., 2017).

Detection of high bromate ion concentrations after ozonation can serve as a cautionary measure and help improve the safety of potable water reuse. The online-monitored data can

be utilized as an indicator of high bromate ion concentrations exceeding the guideline value. However, to date, there are no online analytical methods for bromate.

1.2. Research objectives

The goal of this work was to develop water quality monitoring techniques. Specific objectives of this study are to:

- 1) Identify algae generating odor in water source; and develop and validate an auto-counting technique for the odor-generating algae; and
- 2) Validate the dialysis pre-treatment system with the real-time bacteriological counter in full scale drinking water treatment plant.
- 3) Develop a nanofiltration membrane-based pre-treatment system for continuously analyzing the concentrations of bromate.

1.3. Thesis outlines

The thesis provides a comprehensive literature review about odor in drinking water sources, online bacterial counters, and bromate analysis in Chapter 2. Then, descriptions of water samples, microscope settings, real-time bacteriological counter, dialysis pre-treatment systems, and online bromate analyzer are summarized in Chapter 3. The following chapters include experimental results and discussion. The results regarding the algae auto-counting technique are presented in Chapter 4. Chapter 5 provides the results of the dialysis treatment and the evaluation of the real-time bacterial counter for monitoring a sand filter effluent. Chapter 6 provides the effectiveness of the nanofiltration membrane-based pre-treatment system for online bromate analysis. Chapter 7 provides a summary of the results obtained. Recommendations and suggestions for future research can be found in Chapter 8.

Chapter 2 Literature review

2.1. Odor occurrence in drinking water sources

Avoiding unpleasant odors in drinking water is a major challenge for many water utilities. Although aesthetic issues such as odor do not pose a public health threat, they can violate local water quality regulations and result in a loss of customer trust (Watson, 2004; Winter et al., 2011). According to recent changes in the climate and eutrophication of lakes and reservoirs, algal blooms associated with odor or toxins have occurred more frequently and lasted longer in recent years. Odor in the drinking water supply mainly originates from the presence of geosmin or 2-methylisoborneol (2-MIB) (Faruqi et al., 2018; Kim et al., 1997). These odorous compounds are typically produced by specific cyanobacteria and bacteria in surface water such as lakes and reservoirs (Izaguirre and Taylor, 2004; Lee et al., 2020; Watson et al., 2016) and low populations of specific cyanobacteria as compared to the other algae may be responsible for the occurrence of odor in lakes. A sudden spike of 2-MIB in drinking water sources has often been reported through increased counts of the cyanobacteria, *Pseudanabaena* sp., previously known as *Phormidium tenue*, particularly in East Asia (Kim et al., 2020; Oikawa and Ishibashi, 2004; Rong et al., 2018; Takemoto et al., 2016; Zhang et al., 2016). The *Pseudanabaena* taxon that produces 2-MIB includes *Pseudanabaena* (*P.*) *foetida* v. *foetida*, *P. foetida* v. *intermedia*, *P. foetida* v. *subfoetida*, *P. cinereal*, and *P. yagii*., which are similar in cell dimensions and color (Niiyama et al., 2016a; b; Tuji and Niiyama, 2018).

Odor in drinking water can be reduced by employing additional water treatment processes prior to or following conventional rapid sand filtration systems. Among them, ozone treatment followed by biological activated carbon processes have been successfully implemented for year-round removal of odor in many countries, whereas they require relatively high capital and operating costs. To address infrequent and short-term occurrence

of odor in drinking water sources, water treatment plants (WTPs) typically implement powdered activated carbon (PAC) as a countermeasure for odor removal (Matsui et al., 2007; Srinivasan and Sorial, 2011). However, because PAC doses cannot be adjusted in a timely manner due to a lack of methods for immediately determining odor compound concentrations, a sudden change in odor levels in drinking water sources can result in periods of non-compliance with odor regulations. The analysis of odor compounds (e.g., 2-MIB) at low levels (e.g., regulated concentration of 10 ng/L for drinking water in Japan (Welfare, 2015)) requires a high-performance analytical instrument (e.g., gas chromatograph coupled with mass spectrometer), time-consuming pretreatment, and skilled analysts; thus, it is infrequently conducted (e.g., less than once a day). Although continuous spiking of PAC at high doses during typical odor seasons can minimize the risk of odor issues in the water supply, the high consumption of costly PAC can pose a financial burden on utilities. Alternatively, the frequent analysis of odor-generating algae (e.g., *Pseudanabaena* sp.) concentrations as a surrogate indicator of odor concentrations may allow WTPs to provide timely countermeasures (Bertone et al., 2018; Rousso et al., 2020; Wei et al., 2001).

The automation (or semi-automation) of algal counting methods could allow plant operators without analytical skills to perform frequent on-site quantitative odor analysis. To date, the majority of automated algal counting techniques have been developed based on bright-field microscopy technologies (Embleton et al., 2003; Ernst et al., 2006). Embleton used computer-based image analysis (algorithm) and pattern recognition methods (artificial neural networks) to construct a system to identify, count and measure two cyanobacteria (*Planktothrix agardhii* and *Limnothrix redekei*) and two diatoms (*Aulacoseira subarctica* and *Stephanodiscus astraea*) in lake water. Ernst used fluorescence microscopy and image analysis to develop an automated system to count the cyanobacteria *Planktothrix rubescens* after filtration onto nitrocellulose filters. Another study by Coltelli et al.(2014) established a

counting method based on segmentation and edge detection that attained 98.6% accuracy for 23 different cultivated marine microalgae. However, natural waters, including lake water, contain many non-algal but similar-sized particles that appear in bright-field images, which can cause miscounting. Moreover, the misclassification of algae (e.g. cyanobacteria, diatoms, and green algae) is common for less distinctive filamentous algae (Embleton et al., 2003). The accurate identification of algal class and non-algae particles with similar dimensions remains a major challenge for analysis methods based on microscopic images.

Automated algal counting can be improved by integrating fluorescence information with microscopic image analysis (Bertone et al., 2019; Chang et al., 2012; Ernst et al., 2006; Gregor and Maršálek, 2004). Unlike bright-field images, microscopic imaging under fluorescence can distinguish specific types of algae (Deglint et al., 2019; Hense et al., 2008; Takahashi, 2018). The major source of auto-fluorescent pigments in algae are chlorophyll a and b, which exhibit absorption and emission peaks at approximately 428 nm and 666 nm and approximately 453 nm and 644 nm, respectively (Hense et al., 2008; Schulze et al., 2013; Takahashi, 2018). This feature enables discrimination between algal and non-algal particles during algal counting (Hense et al., 2008; Schulze et al., 2013; Takahashi, 2018). Although several previous studies (Graham et al., 2018; Li et al., 2020) have already used commercial instruments (e.g., Countstar[®] BioMarine or FlowCam[®] Cyano) for auto-counting the specific algae that release the toxin microcystin, no previous studies have established an automated technique for specifically counting odor-producing algae at low concentrations.

This study first assesses the contribution of a specific algae to the occurrence of high 2-MIB concentrations in a drinking water source. Second, this study aims to establish a fluorescence microscopy-based analytical technique for automatically counting the algae to indicate odor. The technique is developed by determining its specific identification criteria (e.g., dimensional conditions and auto-fluorescence) using an image analysis software and

verifying its validity using bright-field microscopic images. To the best of our knowledge, this is the first automatic counting technique that can exclusively count the specific alga *Pseudanabaena* in lake waters.

2.2. Bacterial monitoring during sand filtration

Ensuring the safety of the drinking water is an integral goal for drinking water utilities. To achieve this goal, drinking water from surface water sources is conventionally produced via a so-called rapid sand filtration system, comprising coagulation, flocculation, sedimentation, sand filter, and post-chlorination. A particular focus is placed on microbiological water quality, which can be ensured by attenuating concentrations of microorganisms in water such as pathogenic bacteria and protozoa (i.e., *Cryptosporidium* and *Giardia*) by water treatment processes (WHO, 2011). Therefore, regular monitoring of biological water quality in the drinking water plays a vital role in ensuring microbiological safety. Water authorities in many countries are regulated to periodically evaluate microbiological safety by analyzing culturable indicator bacteria such as *Escherichia coli*. Heterotrophic bacteria can also be analyzed to assess the microbial load. In addition, online instruments measuring surrogate indicators such as turbidity and particle counts are typically equipped in the downstream portion of the sand filter to provide an early warning for sand filter performance or potential contamination. Although the implementation of microbiological sensors or rapid detection methods that can continuously provide the concentration of microorganisms can enhance the safety of drinking water (Lee and Deininger, 1999; Van Nevel et al., 2017), such online microbiological sensors have not been fully established for drinking water applications.

Several online instruments for continuously monitoring bacterial cell concentrations have been recently reported in the literature. (Sherchan et al., 2013; Skovhus and Højris, 2018) For example, an automated flow cytometry coupled with robotics can provide an online profile

for concentrations of intact or cell-damaged bacteria by staining cells with dyes (Besmer et al., 2017; Besmer et al., 2014; Buyschaert et al., 2018; Hammes et al., 2012). A commercial instrument, namely BACTcontrol (MicroLan; Waalwijk, Netherlands), is capable of monitoring specific bacteria such as *E. coli* through the detection of enzymatic activities (Gunnarsdottir et al., 2020; Stadler et al., 2016), BACMON bacteria monitor (GRUNDFOS; Bjerringbro, Denmark) is another commercial instrument that can monitor concentrations of particles using 3D scanning optics in real-time (Højris et al., 2018; Olesen et al., 2018). As one of the real-time bacteria monitoring technologies, we have adopted a real-time bacteriological counter (IMD-WTM, Azbil Corporation; Tokyo, Japan), which counts the concentrations of bacterial particles based on the intensities of scattered light (that recognizes particle sizes relevant to bacteria) and fluorescent light (that can be emitted from bacteria as auto-fluorescence) without any dye additions (Fujioka et al., 2018; Pepper and Snyder, 2016). The capability of real-time bacterial monitoring using the instrument has been previously demonstrated by monitoring sand filter effluent of a drinking water plant and reverse osmosis-treated effluent of a water recycling system (Fujioka et al., 2019a; Fujioka et al., 2019b). However, the relevance of the real-time monitored counts of bacterial particles to other well-established bacterial indicators in drinking water (e.g., heterotrophic plate counts and counts of stained bacteria by fluorescence microscopy) has not been clarified. Identifying the type of bacteria counted by the real-time bacteriological counter is important to establish confidence in the analysis prior to the implementation in drinking water treatment plants.

Other hurdles for implementing real-time bacteriological counters in drinking water applications include the concentrations of impurities in the final product solution. The instrument is based on detecting a weak fluorescent light emitted from bacteria (e.g., riboflavin and nicotinamide adenine dinucleotide hydrogen (NADH)) in addition to their dimensions; thus, any other substances emitting strong fluorescence (e.g., humic acids in

surface water and humic acid-like substances in wastewater) can interfere with the fluorescent light detection of bacteria and exceed the capacity of the fluorescent light detectors (Fujioka et al., 2018). We have recently developed a dialysis membrane-based pre-treatment technique that can remove the interfering constituents without compromising bacterial concentrations in the sample stream (Fujioka and Boivin, 2020b). The dialysis membrane, which has pores (e.g., $<0.005\ \mu\text{m}$ (Sakai, 1994)) smaller than bacterial sizes (e.g., $<0.2\ \mu\text{m}$), allows small constituents such as humic acids to diffuse from the target solution into the dialysate. The dialysate can be regenerated by removing the small constituents with anion exchange resins, thus the pre-treatment system does not require a continuous supply of pure water unlike our previous work (Fujioka et al., 2018). However, the effectiveness of the dialysis membrane-based pre-treatment on the interfering substances has only been assessed in a few hours (Fujioka et al., 2021). The long-term stability in the performance of both dialysis membrane and dialysate regeneration system (i.e., anion exchange resins) is critical to determine its potential for full-scale implementation.

This study aimed to validate the pre-treatment technique and real-time bacteriological counter for monitoring bacterial counts in the sand filter effluent at a full-scale drinking water treatment plant. The performance of the pre-treatment system during real-time monitoring bacteria was evaluated throughout the 20-d operation. The types of bacteria that are monitored by the real-time bacterial counter were evaluated by conventional bacterial counting and 16S rRNA gene sequencing.

2.3. Online monitoring of bromate

Ozonation is a reliable water treatment process that reduces the concentrations of trace organic chemicals and pathogens, such as viruses and bacteria, in water and wastewater, as ozone is a strong oxidant. Therefore, ozonation, followed by treatment with biologically

activated carbon, can be implemented prior to advanced wastewater treatment processes (AWTPs), such as microfiltration or ultrafiltration, reverse osmosis (RO) membrane, and advanced oxidation, for potable use (Pecson et al., 2017; Shi et al., 2021). However, the ozonation of wastewater results in the formation of bromate ions (BrO_3^-), carcinogenic disinfection by-products (DBPs) that are generated from the reaction between ozone and bromide ions in wastewater ($\sim 300 \mu\text{g-Br}^-/\text{L}$) (Jahan et al., 2021), at higher concentrations than the guideline-prescribed value ($10 \mu\text{g-BrO}_3^-/\text{L}$) (Hooper et al., 2020; Vatankhah et al., 2019). Bromate ions are one of the six major contaminants identified in chemical monitoring programs under potable reuse projects which pose a health risk (CSWRCB, 2016). However, thus far, RO membrane treatment has remained as the only reliable process used for the removal of bromate ions from wastewater (Noibi et al., 2020; Tchobanoglous et al., 2015). Therefore, controlling bromate ion formation is a significant challenge for AWTPs without an RO membrane treatment process, which has gained attention as an alternative of RO-based AWTP for potable reuse in inland locations (Bacaro et al., 2019; Dow et al., 2019; Park et al., 2015).

Online monitoring of bromate ion concentrations after ozonation can help improve the safety of recycled water, which will aid the implementation of countermeasures such as reduction of ozone doses up to the guideline-prescribed values. However, the bromate ion concentrations in parts-per-billion ($\mu\text{g/L}$) are analyzed using laboratory-based analytical techniques such as ion chromatography coupled with suppressed conductivity followed by a post-column reaction (Butler et al., 2005; Snyder et al., 2005) and liquid chromatography coupled with tandem mass spectrometry (LC-MS/MS) (Ruffino et al., 2020). Recently, a novel online technology (Ohtomo et al., 2009) based on fluorescence estimation at excitation (EX) and emission (EM) wavelengths of 300 and 400 nm, respectively, has been developed to monitor bromate ion concentration in drinking water. Nevertheless, wastewater contains a

high concentration of dissolved organic compounds that exhibit autofluorescence at 300–400 nm and interfere with the analysis.

The interfering substances in wastewater can be separated from bromate ions using nanofiltration (NF) membranes. Polymeric NF membranes, with a molecular weight cut-off (MWCO) of 200–400 Da (Fujioka et al., 2015; Nghiem et al., 2005), filter out a considerable portion of the organic matter (≥ 500 Da) and a small proportion of bromate ions (10%–50%) (Lin et al., 2020) from water. The NF pre-treatment system coupled with the online elemental analyzer ensures a high rejection rate for interfering substances and a low rejection rate for bromate ions. However, the NF pre-treatment system has not been used with the online bromate ion analyzer. Thus, the efficiency of NF pre-treatment system for the separation of both bromate ions and interfering substances remains to be determined.

The aim of this study was to develop an NF pre-treatment system to enable the continuous monitoring of bromate ion concentrations in treated wastewater by decreasing the permeation of interfering substances. Furthermore, the effects of the pre-treatment conditions on the permeation of interfering substances and bromate ions in the treated wastewater were assessed to maximize the removal of interfering substances. Additionally, the efficiency of the optimized NF pre-treatment system was evaluated by continuously monitoring the bromate ion concentrations in the treated wastewater for three days, and the split samples were analyzed using LC–MS/MS to compare the online-monitored bromate ion concentrations with those obtained via LC–MS/MS.

Chapter 3 Materials and methods

3.1. Algal counting

3.1.1. Water samples

The occurrence of 2-MIB indicated by an increase of *Pseudanabaena* sp. counts was evaluated using a lake in Nagasaki Prefecture, Japan as the drinking water source (denoted as Lake Y). Lake water samples were collected weekly at a V-notch of the lake, which is connected to the water intake of a drinking water treatment plant. The samples were collected from late May to September 2019, and their water quality are summarized in **Table 3.1**.

Table 3.1 Water quality of samples collected from Lake Y (May 24th, 2019 – September 20th, 2019).

Day	Temperature	chlorophyll a	TP	TN	PO ₄ -P	NO ₃ -N	NH ₄ -N	K	Geosmin	2-MIB	pH	Oxidation reduction potential	Electrical conductivity	Dissolved oxygen	Total organic carbon
Unit	°C	µg/L	mg/L	mg/L	mg/L	mg/L	mg/L	mg/L	ng/L	ng/L	—	mV	mS/m	mg/L	mg/L
0	22.8	3.7	0.033	0.396	0.002	0.095	0.018	0.87	0.0	0.0	7.4	240	9.8	7.5	1.40
7	20.0	5.3	0.047	0.535	0.004	0.193	0.037	0.95	0.9	1.3	7.4	204	9.3	7.6	1.54
14	24.2	7.7	0.029	0.354	0.000	0.081	0.012	0.98	1.4	11.3	7.5	217	9.7	7.9	1.53
21	22.8	2.0	0.050	0.200	0.000	0.022	0.000	0.92	2.1	32.8	7.8	214	10.0	8.3	1.97
28	22.7	8.8	0.027	0.393	0.000	0.051	0.013	0.95	1.8	136.5	7.4	174	9.5	7.3	1.64
33	23.2	5.9	0.025	0.335	0.000	0.011	0.022	0.94	1.5	306.1	7.8	213	10.3	8.4	1.64
42	20.4	4.3	0.031	0.628	0.005	0.236	0.053	0.86	0.7	10.4	7.1	236	8.6	6.3	1.56
49	21.4	7.3	0.025	0.484	0.003	0.209	0.018	0.89	0.5	3.3	7.3	221	8.7	7.3	1.60
56	20.5	3.6	0.032	0.738	0.002	0.384	0.010	0.79	0.9	1.9	7.0	239	7.6	7.6	1.47
63	23.0	12.0	0.035	0.641	0.001	0.209	0.019	0.75	0.7	4.6	6.9	214	9.2	6.1	1.47
70	24.0	14.8	0.030	0.434	0.001	0.144	0.033	0.87	0.8	4.4	7.1	219	8.2	7.1	1.43
77	24.8	10.1	0.031	0.469	0.004	0.126	0.046	0.90	1.3	10.2	7.5	221	8.3	7.3	1.65
84	25.6	7.7	0.017	0.387	0.001	0.125	0.048	0.92	1.4	10.4	7.3	198	8.5	6.6	1.46
91	25.5	4.2	0.078	0.854	0.006	0.295	0.030	0.86	1.8	11.1	7.3	194	8.2	6.8	2.05
98	21.2	0.5	0.045	0.843	0.017	0.412	0.032	0.75	2.2	3.5	7.0	225	5.8	8.2	1.40
105	22.5	5.0	0.022	0.683	0.006	0.360	0.013	0.82	1.3	1.1	7.1	219	6.9	7.3	1.15
112	22.5	12.2	0.016	0.484	0.002	0.224	0.036	1.00	1.6	1.1	7.4	211	7.7	8.8	1.23
119	22.0	7.9	0.016	0.343	0.002	0.144	0.089	1.33	1.6	0.6	7.5	209	8.4	7.7	1.10

To develop the auto-counting technique, another lake used as a drinking water source—Lake Kasumigaura (denoted as Lake K), Japan—was selected. The samples were collected at a depth of 0.5 m of Lake K from two different points located in Tsuchiura City (denoted as A and B, **Fig. 3.1**) on four different sampling occasions from September to November 2020, and their water quality are summarized in **Table 3.2**. The samples collected from each lake were stored in the fridge at 4° C and analyzed within four days after sample collection. In addition to the lake water samples, this study used a pure culture of *Pseudanabaena* sp. at a concentration of approximately 10⁴ counts/mL. The pure culture of *Pseudanabaena* sp. was prepared by culturing samples collected from Doshi River (Kanagawa Prefecture, Japan) in a culture medium (10 mg NaNO₃, 1 mg K₂HPO₄, 7.5 mg MgSO₄·7H₂O, 4 mg CaCl₂·2H₂O, 3 mg Na₂CO₃, 0.1 mg FeSO₄·7H₂O, 0.1 mg Na₂EDTA·2H₂O, 100 mL distilled water, and pH 8.0) for 2 weeks.

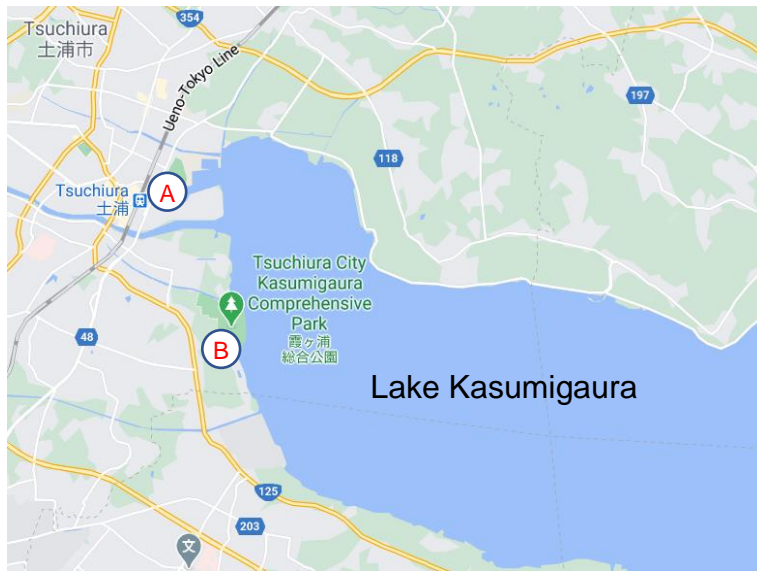


Fig. 3.1 Sampling points A and B of Lake K (created using Google Map).

Table 3.2 Water quality of samples collected from Lake K (29/9/2020 – 16/11/2020). “n.a.” represents data not available.

Date	Code	chlorophyll a ($\mu\text{g/L}$)	Temperature ($^{\circ}\text{C}$)	Electrical conductivity (mS/m)
September 29 th , 2020	1-A	108	22.9	28.3
October 14 th , 2020	2-A	70	21.2	19.9
October 14 th , 2020	2-B	42	21	25.7
November 3 rd , 2020	3-A	148	17.2	23.7
November 3 rd , 2020	3-B	58	17.4	26.5
November 16 th , 2020	4-A	148	n.a.	n.a.
November 16 th , 2020	4-B	94	n.a.	n.a.

3.1.2. *Odor quantification*

The samples collected from Lake Y underwent analysis to detect 2-MIB and geosmin. Each sample was subjected to purge and trap extraction of these compounds using a purge and trap concentrator (PT7000, GL Science, Tokyo, Japan) before analysis with a gas chromatograph–mass spectrometer (GCMS-QP-2010Plus, Shimadzu, Kyoto, Japan). The standards of 2-MIB and geosmin at a concentration of 100 mg/L in methanol were used to create the calibration curve based on their concentrations of 0, 1, 4, 15, 50, and 100 ng/L.

3.1.3. *Microscope and sample preparation*

Both bright-field and fluorescence observations were conducted using an all-in-one Fluorescence Microscope (BZ-X800, Keyence Co.; Osaka, Japan) equipped with an objective lens (Plan Apo λ 20x/0.75; Nikon, Japan) and image processing software installed on a personal computer. Prior to each analysis, a sample volume of 300 μL was placed into a plankton counting polycarbonate slide (MPC-200, Matsunami Glass Industry; Osaka, Japan), which has a specimen capacity of 0.1 mL and chamber depth of 1 mm. The slide containing the sample was inverted for analysis because the objective lens is located underneath the sample stage. Each analysis determined the count of algae in a total sample volume of 23.35

μL . The count of algae was determined based on the natural unit count (units/mL), which may be a single cell, filament, or colony.

3.1.4. Bright-field observation

Bright-field observations were used to manually count algae including *Pseudanabaena* sp., and the bright-field counts were utilized to validate *Pseudanabaena* sp. counts determined by the developed auto-counting method. An image with a total area of 7.78 mm^2 ($2.75 \text{ mm} \times 2.83 \text{ mm}$) was created by automatically attaining 35 segmented images under bright-field condition. The counts of different types of algae in the segmented images were manually recorded. It should be noted that image acquisition of algae under bright-field or fluorescence observations was performed at the same location on the sample slide to accurately compare the observed algae.

3.1.5. Fluorescence observation

Fluorescence observations were performed using a custom-made long-pass optical filter (Chroma Technology Japan; Yokohama, Japan), which has excitation and emission wavelengths of $440 \pm 20 \text{ nm}$ and $\geq 590 \text{ nm}$, respectively (**Fig. 3.2**). This optical filter covers the absorption and emission peak of auto-fluorescent compounds in algae: chlorophyll a (approximately 428 nm and 666 nm , respectively) and chlorophyll b (approximately 453 nm and 644 nm , respectively). Therefore, algae cells are displayed in red, whereas algae cells with a fluorescence intensity higher than a preset threshold are displayed in white (or blue in microscope haze reduction mode). The image acquisition of each sample was conducted with a fluorescence exposure time of 0.2 s and the microscope haze reduction mode was set to 5. The haze reduction mode removes the blur inherent to fluorescence without artefacts. Fluorescent objects that exhibited brightness above a threshold value were recognized as algae. Algae in each sample were analyzed in terms of their dimensions (e.g., width and

length) and fluorescence intensity. Subsequently, unique properties of the targeted 2-MIB-producing algae were determined, and they were used as pre-set object properties in the following method development.

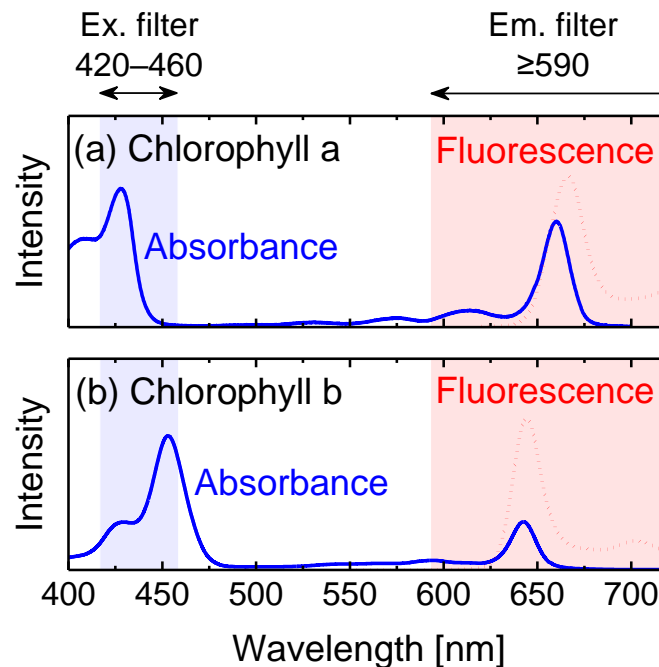


Fig. 3.2 Absorbance and fluorescence emission spectra of (a) chlorophyll a and (b) chlorophyll b, as well as the excitation (Ex) and emission (Em) ranges of the selected optical filter. Chlorophyll spectra were obtained from PhotochemCAD™ (<http://www.photochemcad.com>).

3.1.6. Auto-counting method development and validation

Fluorescence observations were used to develop the auto-counting method.

Step 1: An image with a total area of 7.78 mm² (2.75 mm × 2.83 mm) was created by automatically attaining 35 segmented images, each of which was captured in auto-focus and auto-moving stage mode.

Step 2: Using hybrid cell count software (BZ-H3C, Keyence Co.; Osaka, Japan), the characteristics of each algae were analyzed, and they were sorted based on their dimensions

(e.g., width and length) and fluorescence intensity. Thereafter, the software extracted only the target algal cells with pre-set object properties (i.e., length, width, and fluorescence intensity) of the targeted 2-MIB-producing algae. Analysis of each sample was performed in triplicate and the average count and count ranges of each algae were calculated.

The validity of the auto-counting method was evaluated by assessing a correlation between manual counts (in bright-field observation) and automatic counts (in fluorescence observation) of the 2-MIB-producing algae in Lake K samples in the corresponding images.

3.2. Online bacterial counting

3.2.1. The sand filtration process

This study was conducted using a full-scale conventional rapid sand filtration system located at a drinking water treatment plant in Nagasaki, Japan. The rapid sand filtration system included several basins in the following sequence: a water intake, two rapid mixing, two flocculation and sedimentation, six sand filter, and post-chlorination. Chlorination was also performed prior to the sand filter basins for mitigating algal and bacterial growth. Sand filter basin was based on two filter media layers: anthracite (depth = 0.3 m, effective size = 1.2 mm, and uniformity coefficient = 1.4) and fine sand (depth = 0.35 m, effective size = 0.6 mm, and uniformity coefficient = 1.4). The plant was fed with river and lake water as drinking water sources. The rapid sand filtration system was operated by dosing a poly-aluminum chloride at 32–44 mg/L and performing an intermediate chlorine dose of 1.0–1.5 mg/L at the exit of the sedimentation basins (i.e., prior to the sand filter basins). Backwashing of each sand filter basin was conducted routinely every three days. Each backwashing process required approximately 40 min until the filtration was resumed: (1) water level drop process (10 min), (2) surface washing (4 min), (3) backwashing (10 min), discharge of backwashed water (2 min), and (5) inflow of feed solution (10 min). After backwashing, the inflow rate of

the sand filter basin was step-wisely increased until the pre-set flow rate. Filtrate of a sand filter basin was continuously collected from a filtrate pipe and transferred through an approximately 1.5 m Polytetrafluoroethylene (PTFE) tube (1/8" and 1/16" outer and inner diameter, respectively) to the dialysis-based pre-treatment system followed by the real-time bacteriological counter.

3.2.2. Dialysis membrane-based pre-treatment system

Prior to the real-time bacteriological counter, sand filter effluent was treated with a pre-treatment system. The pre-treatment system comprises a hollow fiber polyethersulphone dialysis membrane module (Diyalizerler Polynephron™ PES-25Dæco, Nipro, Osaka, Japan) with an effective membrane area of 2.5 m², two smooth-flow pumps before and after the membrane module (Q100, Tacmina; Osaka, Japan), a diaphragm pump for recirculating the dialysate (DCP 6800, Aquatec International, Inc.; Irvine, CA, USA), two parallel glass columns containing anion exchange resin (AER) A502 PS (150 mL) or A860 (150 mL) (Purolite K. K.; Tokyo, Japan), and a 5-L dialysate reservoir (**Fig. 3.3**). All components in the pre-treatment system were interconnected with PTFE tubes. The dialysate, the solution used for removing interference substances in the sample solution via dialysis membrane, was recirculated through the external hollow fibers at a flow rate of 0.5 L/min and was regenerated through the columns of AER that are capable of removing dissolved organic matter. The sand filter effluent went through the internal hollow fibers, where constituents smaller than the membrane pore size diffused through the dialysis membrane, at a flow rate of 11.5 mL/min. The pre-treated sand filter effluent was fed to the real-time bacteriological counter at a flow rate of 10.0 mL/min, while the rest (i.e., 1.5 mL/min) was continuously drained for manual sampling. Manual sampling was conducted periodically for epifluorescent

bacterial counts and plate counts analysis. The residual chlorine (0.3–0.6 mg-Cl₂/L in the filtrate) was quenched with sodium thiosulphate in the sterile sample bottles.

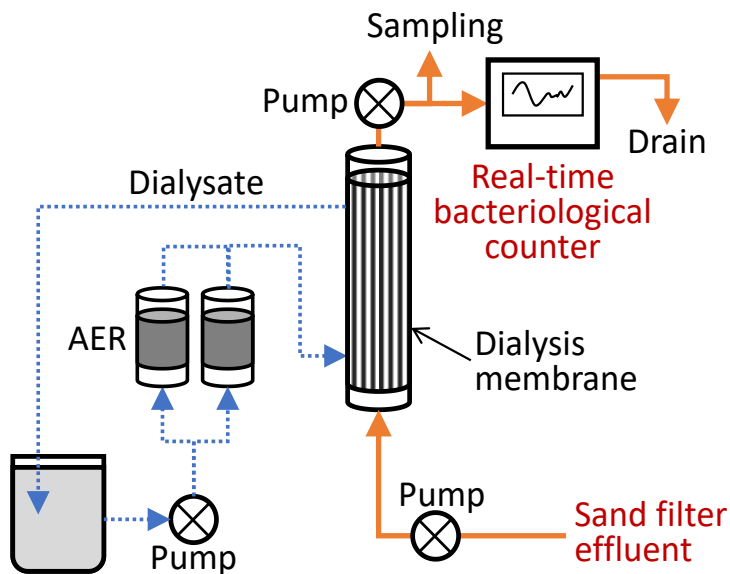


Fig. 3.3 Schematic diagram of the online dialysis membrane pre-treatment system coupled with a real-time bacteriological counter.

3.2.3. *Real-time bacteriological counter*

Bacterial particle counts in the sand filtrate were monitored online using a real-time bacteriological counter (IMD-WTM, Azbil Corporation; Tokyo, Japan). The instrument determined bacterial or non-bacterial particles based on the intensity of scattered and fluorescence light (**Fig. 3.4**). Each particle in the flow channel was first exposed to light with an excitation (Ex) wavelength of 405 nm. A scattered light detector in the instrument measures the intensity of scattered light, which determines each particle dimension. Further, two fluorescence light detectors measure the intensity of fluorescence light at 415–450 and 490–530 nm, which correspond to auto-fluorescence emitted from the riboflavin and NADH of bacteria. Particles with dimensions equivalent to bacteria (e.g., >0.5 μm) and with a pre-set fluorescence intensity were recognized as bacteria, and their number was counted every 1 s.

The instrument had a bacterial particle detection range of 1–50,000 counts/mL. The dialysis-based pre-treatment system functioned to attenuate the concentration of background interfering substances (e.g., dissolved humic acid-like substances) that emit high intensity of light at the fluorescence light detectors. The background interfering substances in the dialysate was removed by AER resins during recirculation.

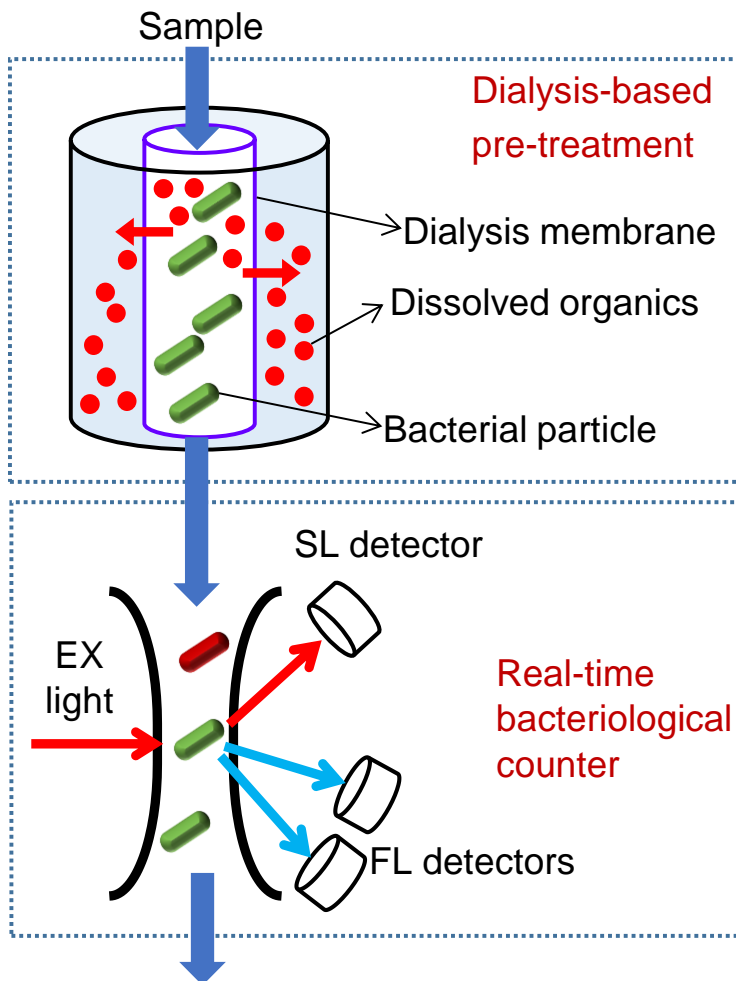


Fig. 3.4 Conceptual diagram of the real-time bacteriological counter involving scattered light (SL) and fluorescent light (FL) and the dialysis-based pre-treatment system.

3.2.4. Manual bacterial counts

Bacterial counts were determined using a fluorescence microscope (BZ-X800, Keyence Co.; Osaka, Japan). Total bacteria counts were measured using three different stains, such as

acridine orange (AO) (Dojindo Laboratories; Kumamoto, Japan), SYTOTM9 of Live/DeadTM BacLightTM Bacterial Viability kit (Thermo Fisher Scientific; Waltham, MA, USA), or SYBR[®] green I (Takara Bio; Kusatsu, Japan). Live bacterial counts were calculated by subtracting the dead/damaged bacterial counts measured with propidium iodide (PI) stain from the total counts. PI solutions used in this study were purchased from Dojindo Laboratories (Kumamoto, Japan) or Thermo Fisher Scientific (Waltham, MA, USA).

When AO and PI were used, each 1 mL sample was stained with 3 μ L of AO solution. After 5 min of incubation, 1 μ L of the PI solution was added as a counterstain and the sample was incubated for 5 min. When Live/DeadTM BacLightTM Bacterial Viability kit was used, each 1 mL sample was stained with 1.5 μ L of SYTOTM9 and 1.5 μ L of PI and was incubated for 15 min. As for SYBR[®] Green I, each 1 mL sample was stained for 15 min with 2 μ L of the SYBR[®] Green I working solution (1:5000 final concentration), which was prepared by diluting 2 μ L of SYBR[®] Green I with 8 μ L of pure sterile water. All sample incubations were conducted in the dark at approximately 23 °C. After incubation, 500 μ L of the stained sample was filtered through a 0.2 μ m pore size track-etched polycarbonate microfiltration (MF) filter (Merck; Tokyo, Japan). Thereafter, each MF filter was analyzed using a green filter (excitation wavelength = 470 ± 40 nm, absorption wavelength = 525 ± 50 nm) and a red filter (excitation wavelength = 545 ± 25 nm, absorption wavelength = 605 ± 70 nm). A total of 20 images was taken and analyzed for each repetition. Each analysis was duplicated.

Viable bacteria counts were determined by using the heterotrophic plate counts method. 0.5 mL sample water was spread on R2A plates (Nissui Pharmaceutical; Tokyo, Japan) and incubated at 35 °C for 7 d before enumeration. The assays were triplicated.

3.2.5. Bacterial community analysis

Bacteria measured by the real-time counter were assessed by analyzing bacterial communities in the sand filter effluent. Bacterial biomass was collected by filtering 15 L of the sand effluent water with a track-etched polycarbonate MF filter (0.2 μm pore size and 47 mm diameter; Merck, Tokyo, Japan) on days 5 and 12. Analysis with 16S rRNA gene sequencing was conducted at Hokkaido System Science (Sapporo, Japan). The details of the method can be found in our previous study (Fujioka and Boivin, 2020a). Briefly, DNA was extracted using the Extrap Soil DNA Kit Plus ver.2 (Nippon Steel Eco-Tech Corporation; Tokyo, Japan). The samples were amplified by a first-stage PCR. After purification, a second PCR was realized with dual indices and Illumina sequencing adaptors using the Nextera XT Index Kit. After purification, the final products were sequenced by Illumina MiSeq (Illumina K.K., Tokyo, Japan). The QIIME2 bioinformatics pipeline was used for cluster generation.

3.2.6. Excitation emission matrix spectrum

Changes in the concentrations of interfering substances before and after the pre-treatment system were evaluated through fluorescence intensity at an excitation wavelength of 405 nm with an RF-6000 spectrophotometer (Shimadzu Co., Kyoto, Japan).

3.3. Online monitoring of bromate

3.3.1. Materials

The standard solution of bromate ions (2,008 mg BrO_3^-/L) was obtained from FUJIFILM Wako Pure Chemical Corp. (Osaka, Japan), and a bromate stock solution (1 mg/L) was prepared in pure water. Trifluoperazine dihydrochloride (TFP) was obtained from Tokyo Chemical Industry Co. Ltd. (Tokyo, Japan), and a TFP stock solution (150 $\mu\text{mol}/\text{L}$) was prepared in pure water. Membrane bioreactor (MBR)-treated wastewater samples, produced

using hollow fiber ultrafiltration membranes with a nominal pore size of 0.05 μm , were collected from a municipal wastewater treatment plant in Japan. In addition, samples of effluent produced through primary wastewater treatment (i.e., screens followed by sedimentation) were collected at another municipal wastewater treatment plant in Japan.

3.3.2. Analytical methods

Bromate ion concentrations were determined using a prototype online bromate ion analyzer (METAWATER Co. Ltd., Tokyo, Japan) based on the changes in fluorescence intensities, resulting from the reaction between TFP and bromate ions.(Ohtomo et al., 2009) The overall procedure is depicted in **Fig. 3.5**. First, approximately 150 mL auto-collected wastewater samples, which were subjected to acidification with 0.5 M HCl, were mixed with 3.0 μM TFP stock solution for 1 min. Subsequently, fluorescence intensities were estimated at EX and EM of 300 nm and 400 nm, respectively. Second, the wastewater samples were analyzed via a method similar to the abovementioned method, using 10 $\mu\text{g/L}$ of bromate ions. The bromate ion concentrations were then determined using the fluorescence intensity estimates of the two analyses (that is, with and without the bromate ion standard solution). Each analysis duration was 90 min, and a sample volume of approximately 450 mL was used. A standard curve was generated using bromate solutions (in pure water) with concentrations of 0, 2.5, 5.0, and 10 $\mu\text{g/L}$.

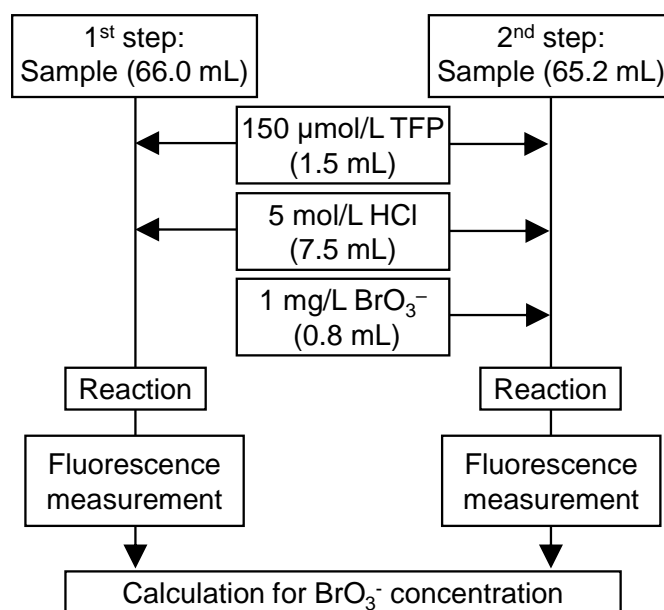


Fig. 3.5 Flow diagram of the online process used to determine bromate ion concentration.

Bromate ion concentrations in the manually-collected samples were determined using LC-MS/MS (ACQUITY UPLC system and ACQUITY TQD MS/MS, Waters Co.; Milford, MA, USA) equipped with an ACQUITY UPLC BEH Amide column (2.1 × 150 mm, 1.7 µm, Waters Co.; Milford, MA, USA) (Table 3.3). Water samples were diluted with acetonitrile (LC-MS grade, FUJIFILM Wako Pure Chemical; Osaka, Japan) since the BEH Amide is a hydrophilic interaction chromatography column, and an 80/20 (v/v) mixture of acetonitrile and the water sample was injected into the analytical system. A binary gradient with a flow rate of 0.3 mL/min was used. The mobile phases A and B were 50 mM ammonium formate and acetonitrile, respectively. The mass spectrometer was operated using electrospray ionization in negative ion mode. Multiple reaction monitoring (MRM) mode was used to quantify ions in the samples, with precursor and product ion transitions corresponding to 127 m/z and 111 m/z, respectively. Moreover, the concentrations of the interfering substances in the wastewater samples were characterized using the excitation–emission matrix (EEM) spectra obtained using the RF-6000 spectrophotometer (Shimadzu Co., Kyoto, Japan).

Table 3.3. LC-MS/MS conditions for bromate analysis.

Parameters	Conditions
Column temperature	40°C
Injection volume	10 µL
Gradient conditions	B: 5% (0 min) → 5% (0.5 min) → 60% (5 min) → 60% (8 min) → 5% (9 min)
Capillary voltage	0.5 kV
Cone voltage	20 V
Collision energy	17 V for m/z 126.8>110.9 and 20 V for m/z 126.8>94.9
Source temperature	120°C
Desolvation temperature	400°C
Desolvation gas flow	600 L/h
Cone gas flow	50 L/h
Multiple ion monitoring	m/z 126.8>110.9 (quantification) m/z 126.8>94.9 (confirmation)

3.3.3. *The NF pretreatment system*

Spiral-wound polyamide NF membrane elements (NF270-1812-250; Pure-Pro Water Corporation, Kaohsiung, Taiwan; effective membrane area = 0.6 m²) were installed in an NF pre-treatment system (**Fig. 3.6**) to separate the interfering substances from the bromate ions. The NF membrane elements were assembled using the NF membranes (NF270, DuPont Water Solutions, Wilmington, DE, USA) with an MWCO of 300 Da, according to the manufacturer's instructions.

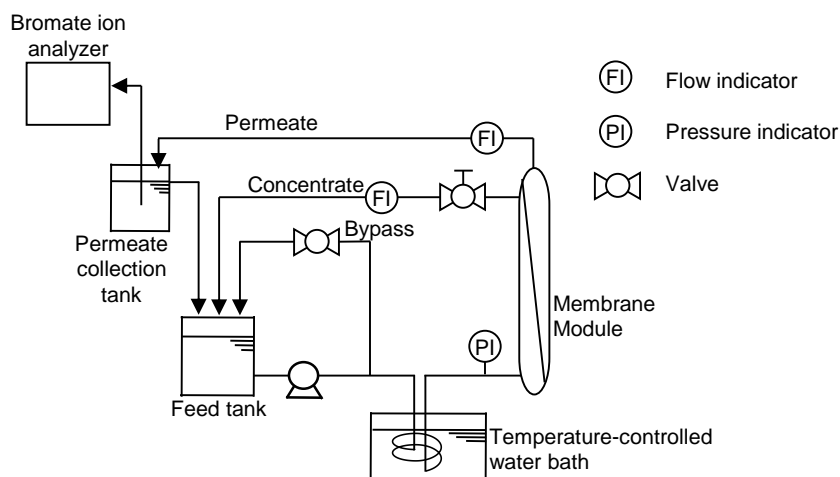


Fig. 3.6 Nanofiltration (NF) pre-treatment system diagram with a spiral-wound NF270 membrane element. An NF membrane element housed in a membrane housing was called as a membrane module. The NF pre-treatment system comprised of a membrane module, a diaphragm pump (DCP 8800, Aquatec International, Inc., CA, USA), flow indicators, a pressure gauge, a 22.5 L feed tank, a 300 mL permeate collection tank equipped with an over-flow pipe, and a coil pipe connected to a temperature-controlled water bath (Thermax Water Bath, TM-1A, AS-ONE, Osaka, Japan).

3.3.4. *Experimental protocols*

Prior to each test, the NF pre-treatment system with the NF membrane module was conditioned by conducting filtration of pure water for two days. After replacing pure water with 22.5 L of MBR-treated wastewater, the rate of inflow to the membrane module was set at 700 mL/min. The permeate flux and feed temperature were adjusted to 1–10 L/m² h and 10–35 °C, respectively. The bromate stock solution was added into the feed tank in a stepwise manner from 0 µg/L to 12 µg/L, and the permeate was collected in an equipped collection tank. The permeate was transferred from the collection tank to the online bromate ion analyzer using a 1/8" polytetrafluoroethylene pipe. Both the permeate and the concentrate were recirculated during the test period. The entire volume of the feed was replaced after 1.3

and 2.8 d. Feed and permeate samples collected from the feed and permeate collection tanks, respectively, were manually analyzed using LC–MS/MS and the RF-6000 spectrophotometer. When bromate ion concentrations were analyzed in the primary wastewater treatment effluent samples, the permeate flux and feed temperature during the NF pre-treatment were adjusted to 1 L/m² h and 35 °C, respectively. A bromate stock solution was added into the primary wastewater treatment effluent at a concentration of 4 µg/L.

Chapter 4 Algal counting

4.1. Identification of an odor-producing algae

Prior to development of the auto-counting technique, the relationship between the presence of odor (i.e., 2-MIB) and growth of algae was assessed using a total of 18 samples, which were collected weekly from Lake Y. At 7 d, a 2-MIB concentration of 1.3 ng/L was observed which continuously increased until peaking (306 ng/L) at 33 d (**Fig. 4.1a**). Similarly, *Pseudanabaena* sp. first appeared at 10 units/mL at 7 d and rapidly increased to 530 units/mL at 28 d. Thereafter, *Pseudanabaena* sp. counts peaked (1,700 units/mL) at 33 d (**Fig.4.1b**). Notably, *Pseudanabaena* sp. accounted for 8% of total algae counts (21,560 units/mL) at their peak. At 42 d, the occurrence of both 2-MIB and *Pseudanabaena* sp. both ceased. The region of Lake Y entered the rainy season after 33 d, and precipitation lasted throughout the following week until 42 d (**Fig. 4.2**), which may have flushed any surface water containing 2-MIB and *Pseudanabaena* sp. from Lake Y. No other 2-MIB-producing cyanobacteria were identified during this period (**Table 4.1**). The concurrent changes in 2-MIB and *Pseudanabaena* sp. in Lake Y resulted in a notable correlation (**Fig. 4.3**), whereas counts of other algae did not show any clear correlations with 2-MIB concentrations. Therefore, the growth of *Pseudanabaena* sp. was most likely associated with the occurrence of 2-MIB in Lake Y during this assessment period. Similar weekly investigation was conducted for Lake Y from April to October 2020, where neither odor (2-MIB) nor *Pseudanabaena* sp. was confirmed.

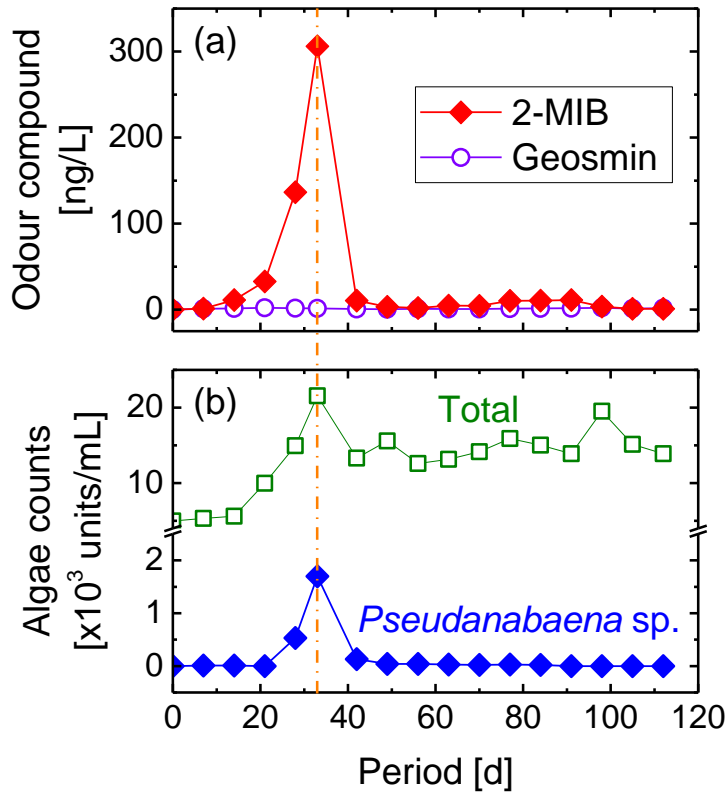


Fig. 4.1 (a) Concentrations of 2-MIB and geosmin, and (b) total algae and *Pseudanabaena* sp. counts in Lake Y quantified via bright-field observations between the 24th of May and the 20th of September 2019.

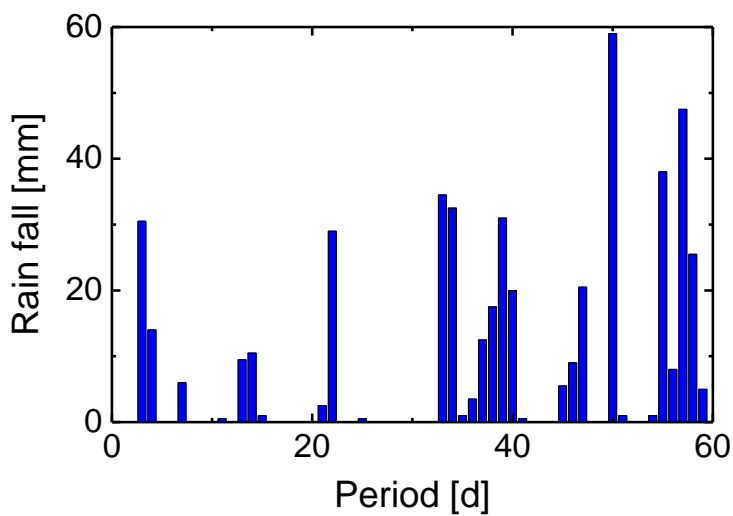


Fig. 4.2 Rainfall during the assessment of Lake Y from the 24th of May 2019.

Table 4.1 Algae population (units/mL) in Lake Y in 2019.

Date	24/05	31/05	07/06	14/06	21/06	26/06	05/07	12/07	19/07	26/07	02/08	09/08	16/08	23/08	30/08	06/09	13/09	20/09	
Day	0	7	14	21	28	33	42	49	56	63	70	77	84	91	98	105	112	119	
Cyanobacteria																			
<i>Anabaeana</i>	0	0	0	0	0	0	0	0	0	0	0	0	0	0	0	0	0	0	0
<i>Anabaena affinis</i>	0	0	0	0	0	0	0	0	0	0	0	0	0	0	0	0	0	0	0
<i>Alphanocapsa</i>	0	0	0	0	0	0	0	0	0	0	0	0	0	0	0	0	0	0	0
<i>Chroococcus</i>	0	0	0	0	0	0	0	0	0	0	0	0	0	0	0	0	0	0	0
<i>Pseudanabaena limnetica</i>	0	0	0	0	0	0	0	0	0	0	0	0	0	0	0	0	0	0	0
<i>Pseudanabaena sp.</i>	0	10	10	0	530	1700	130	40	40	30	20	30	20	0	0	0	0	0	0
<i>Microcystis viridis</i>	0	0	0	0	0	0	0	0	0	0	0	0	0	0	0	0	0	0	0
<i>Microcystis aeruginosa</i>	0	0	0	0	0	0	0	0	0	0	0	0	0	0	0	0	0	0	0
Others (unicellular cyanobacteria)	4800	4750	3750	8400	12300	19000	11600	12400	11600	12300	13100	12500	13500	13100	19500	14800	12700	13000	
Diatoms																			
<i>Cyclotella</i>	70	0	20	110	0	0	70	20	120	110	300	2570	150	80	0	80	360	170	
<i>Aulacoseira granulata</i>	0	0	0	0	0	0	0	10	0	20	30	20	0	0	0	0	20	0	
<i>Aulacoseira g var ang f spiralis</i>	0	0	0	0	0	0	0	10	0	0	0	10	0	0	0	0	10	0	
<i>Aulacoseira distans</i>	0	0	0	0	0	0	0	0	0	0	0	0	30	20	0	0	640	190	
<i>Attheya zachariasii</i>	0	0	0	0	0	0	0	0	0	0	0	0	220	60	0	0	0	0	
<i>Fragilaria crotonesis</i>	0	0	0	0	10	0	0	0	0	20	60	20	0	0	0	0	0	0	
<i>Synedra acus</i>	0	0	40	10	0	0	0	0	0	30	50	30	0	0	0	0	10	60	
<i>Navicula</i>	10	60	80	270	140	150	210	800	100	100	70	80	0	10	0	60	10	10	
<i>Nitzschia</i>	10	0	0	0	0	0	0	0	0	0	0	0	0	0	0	0	0	0	
<i>Melosira varians</i>	0	0	0	10	0	0	0	0	0	0	0	20	0	0	0	0	0	0	
<i>Cymbella</i>	0	0	40	10	0	20	0	0	0	0	10	0	10	0	0	0	0	0	
Others	0	0	90	0	0	0	360	0	0	10	0	0	0	0	0	30	0	0	
Green algae																			
<i>Chlamydomonas</i>	10	60	110	20	30	0	30	50	80	180	70	50	90	110	0	30	30	50	
<i>Pleodorina</i>	0	0	0	0	0	0	0	0	0	0	0	0	40	0	0	0	0	0	
<i>Sphaerocystis schroeteri</i>	0	0	0	0	90	0	0	0	0	30	0	0	50	190	0	0	0	160	
<i>Oocystis</i>	0	70	40	0	30	20	0	0	10	0	0	0	170	0	0	0	0	0	
<i>Golenkinia radiata</i>	0	0	0	0	0	0	20	20	0	0	0	0	0	0	10	0	0	0	
<i>Micractinium pusillum</i>	0	20	20	0	0	0	0	0	0	0	0	0	0	0	0	0	0	0	
<i>Staurastum</i>	0	0	0	10	0	0	0	0	0	10	0	0	0	0	0	0	0	0	
<i>Scenedesmus</i>	0	20	150	310	390	210	800	2090	440	100	40	70	20	0	0	0	40	0	
<i>Coelastrum cambricum</i>	0	0	20	30	0	0	0	40	0	0	0	0	0	0	0	0	30	0	
<i>Cosmarium</i>	0	0	10	0	0	0	0	0	0	20	0	0	0	20	10	0	0	0	
<i>Pediastrum duplex</i>	0	0	0	0	0	0	0	0	0	0	0	0	40	0	0	0	0	0	
<i>Crucigenia</i>	0	0	50	0	0	0	0	0	0	0	0	0	0	0	0	0	0	0	
<i>Gleocystis</i>	0	30	0	480	0	10	0	0	0	0	0	0	120	20	0	0	0	0	
<i>Ankistrodesmus</i>	0	0	0	40	70	20	50	30	30	0	0	0	250	0	0	0	0	0	
<i>Eudorina</i>	0	0	10	10	0	0	10	0	0	50	190	390	310	0	0	0	10	30	
<i>Spondylosium</i>	0	0	0	0	0	0	0	0	0	0	0	20	0	0	0	0	0	0	
<i>Dictyosphaerium</i>	0	0	0	0	0	0	0	0	0	0	0	0	0	0	0	0	20	10	
Others	30	70	760	210	1300	430	0	50	120	150	210	50	160	20	0	100	20	50	
Others																			
<i>Mallomonas akrokomos</i>	0	0	10	0	0	0	0	0	0	0	0	0	0	0	0	0	0	0	
<i>Mallomonas caudata</i>	0	60	70	0	0	0	0	0	40	0	10	0	0	10	0	0	0	0	
<i>Mallomonas tonsurata</i>	0	0	200	0	0	0	0	0	0	0	0	0	0	0	0	0	0	0	
<i>Botryococcus braunii</i>	0	0	0	0	30	0	0	0	0	0	10	0	0	0	0	0	0	0	
<i>Ceratium</i>	0	10	10	10	0	0	0	0	0	0	0	0	0	10	0	0	0	0	
<i>Trachelomonas</i>	60	170	120	40	20	0	40	30	20	30	10	10	0	60	10	20	0	10	

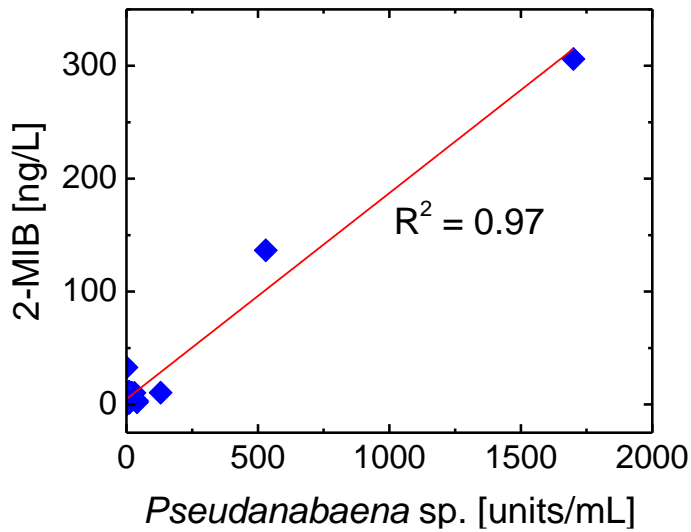


Fig. 4.3 Correlation between *Pseudanabaena* sp. and 2-MIB concentrations in Lake Y.

The concurrent annual occurrence of both 2-MIB and *Pseudanabaena* sp. has been annually reported in other lakes. (Kajino and Sakamoto, 1995; Sugiura et al., 1998; Yagi et al., 1983) The results of this study confirmed that 2-MIB issues in Lake Y are similar to those in other major lakes. Throughout the assessment period, a drinking WTP using Lake Y water as an input maintained relatively high PAC doses of 5–20 mg/L (**Fig. 4.4**) to precautionarily address the spike of 2-MIB because 2-MIB was being analyzed only once per week. Frequent on-site analysis of *Pseudanabaena* sp. counts using an auto-counting technique may be able to provide early detection of potential odor occurrence and help minimize PAC doses.

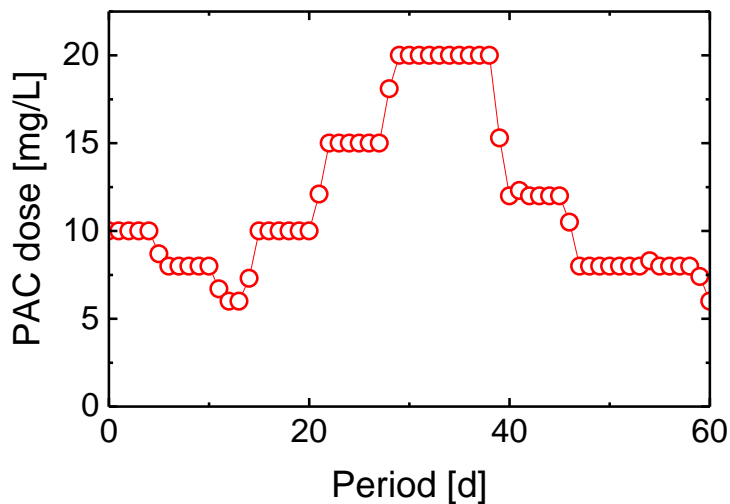


Fig. 4.4 Powdered activated carbon (PAC) doses at the drinking water treatment plant during the assessment of Lake Y.

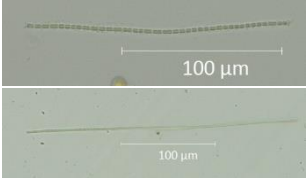
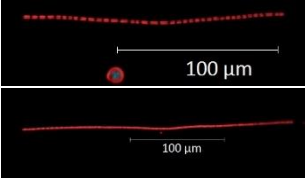
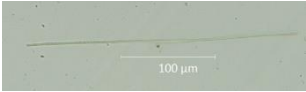
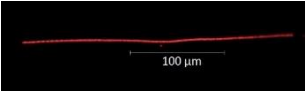
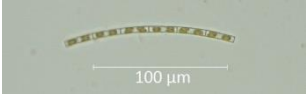
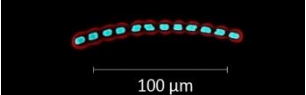


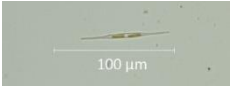
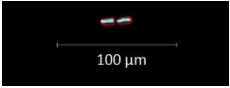
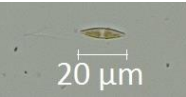

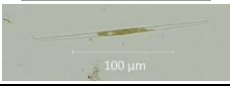
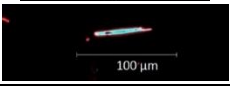


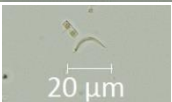

4.2. Automated counting technique development

4.3. Fluorescence observations

To establish the criteria for the automatic identification and quantification of *Pseudanabaena* sp. in lake water, the dimensions and fluorescence intensity of each algae were assessed through fluorescence observations of the first samples collected from Lake K. Types of algae cannot be clearly identified under fluorescence observations; thus, each algae under fluorescence observation was cross-checked using bright-field observation in the corresponding image. It is noted that Lake Y was not used here because neither 2-MIB nor *Pseudanabaena* sp. were identified in Lake Y from April to October 2020. In general, the size of cyanobacteria such as *Pseudanabaena* sp. in the bright-field observations was equivalent to that in the fluorescence observations because chlorophyll is uniformly present throughout the cell of cyanobacteria (**Table 4.2**). Each *Pseudanabaena* sp. unit consists of one or more cells; thus, a large variation in the fluorescence-observed length of

Pseudanabaena sp. was observed. It is noted that although the joints connecting *Pseudanabaena* sp. cells have no chlorophyll, appearing as a short black gap in fluorescence images, they were recognized as a solid unit by the software. The *Pseudanabaena* sp. in Lake K showed a large length variation ranging from 10–207 μm (average 48.5 μm). In contrast, the width of *Pseudanabaena* sp. was relatively uniform, with a range of 2.0–6.5 μm (average 3.8 μm). Notably, the light emitted from out-of-focus regions in algal cells cannot be displayed with a blurred image; thus, the dimensions of algal cells observed under fluorescence observation can be slightly larger than those under bright-field observation. The results indicate that the length of *Pseudanabaena* sp. can vary considerably depending on individual units; however, the length (≥ 15 μm) and width (2.0–6.5 μm) of *Pseudanabaena* sp. can be used as criteria for distinguishing *Pseudanabaena* sp. from other algae. Note that the length of ≥ 15 μm (rather than ≥ 10 μm) was determined as the threshold in order to exclude short and thin green algae with weak fluorescence intensity. Among other cyanobacteria, *P. limnetica* exhibited a similar shape and color, whereas its length and width were generally greater than those of *Pseudanabaena* sp., which can be used to eliminate most *P. limnetica* from the auto-counted algae. The observed cyanobacteria other than *Pseudanabaena* sp. and *P. limnetica* were not filamentous.

Table 4.2. Images and properties of algae: *Pseudanabaena* sp. and other algae that have similar dimensions.

Name	Bright-field observation Image	Fluorescence observation				
		Image	Length ^a [μm]	Width ^a [μm]	Color ^c	Number ^b
Cyanobacteria						
<i>Pseudanabaena</i> sp.			48.5 ± 48.9	3.8 ± 1.1	red	40
<i>P. limnetica</i>			199 ± 67	7.6 ± 1.8	red	20
Diatom						
<i>Aulacoseira italica</i>			24.9 ± 18.5	6.0 ± 2.1	blue & red	10
<i>Aulacoseria granulata</i>			363 ± 228	24.5 ± 13.4	blue & red	13
<i>Nitzschia</i>			21.3 ± 6.1	6.1 ± 2.4	blue & red	10
<i>Navicula</i>			15.0 ± 3.6	5.2 ± 0.7	blue & red	5
<i>Synedra</i>			52 ± 17	6.3 ± 1.2	blue & red	3
Green algae						
<i>Schroederia</i>			15.8 ± 2.5	5.3 ± 1.4	blue & red	6
<i>Ankistrodesmus</i>			14.2 ± 2.1	3.8 ± 0.4	blue & red	10

^aAverage and standard deviation, and ^btested number of algae for quantification of their dimensions. ^cColor on the image after reduction of fluorescence haze by the software

Diatoms and green algae that exhibited a similar shape to *Pseudanabaena* sp. are listed in **Table 4.2**. Because a similar shape can cause a misidentification during auto-counting of *Pseudanabaena* sp., the identification of distinct features becomes important for auto-counting. In the bright-field observations, *Pseudanabaena* sp. exhibited a green color due to the presence of chlorophyll throughout the cell, whereas diatoms and green algae exhibited green chloroplasts containing chlorophylls and other pigments that were densely distributed in a spotted pattern (Millie et al., 2010). In the fluorescence observations, several diatoms such as *Nitzschia*, *Navicula*, and *Aulacoseira (A.) italica* appeared in similar dimensions to the short units of *Pseudanabaena* sp. due to the position of their chloroplasts. It is noted that the length of *A. italica* ($>100\ \mu\text{m}$ in bright-field observations) appeared shorter in the fluorescence observations ($24.9 \pm 18.5\ \mu\text{m}$) due to the relatively long gap between chloroplasts in their units. However, the width of *Navicula* and *A. italica* was generally wider than that of *Pseudanabaena* sp. More importantly, the chlorophyll contained in the chloroplasts of all diatoms and green algae in this study emitted intense auto-fluorescence, exceeding a preset threshold of fluorescence intensity of the fluorescence microscope. As a result, their chloroplasts appeared as a white-blue color on the images after the software reduced the fluorescence haze. Cyanobacteria appeared red on the images. The difference in fluorescence intensity among the algae enabled the microscope software to discriminate diatoms and green algae from cyanobacteria, including *Pseudanabaena* sp.

Using the fluorescence information of each algae (**Table 4.2**), an automatic technique for determining *Pseudanabaena* sp. counts was established (**Fig. 4.5**). First, each sample was subjected to an image acquisition step under fluorescence, and each fluorescent object in the captured image was automatically sorted based on their properties (e.g., dimensions and fluorescence intensity) by the cell counting software. Second, all fluorescent objects with a length of $\geq 15\ \mu\text{m}$, width of $2.0\text{--}6.5\ \mu\text{m}$, and fluorescence intensity below the threshold were

automatically counted as *Pseudanabaena* sp. Overall, the developed method was found to require approximately 60 min to conduct triplicated analysis after sampling after placing the plankton counting polycarbonate slide on the stage of the fluorescence microscope: image acquisition and auto-counting steps can be completed within a total of 50 min, and manual processing of image selection on the computer screen can be completed within a total of 10 min. The manual processing does not require analytical skills of workers, which is advantageous over the conventional algae manual counting methods under the bright-field observation.

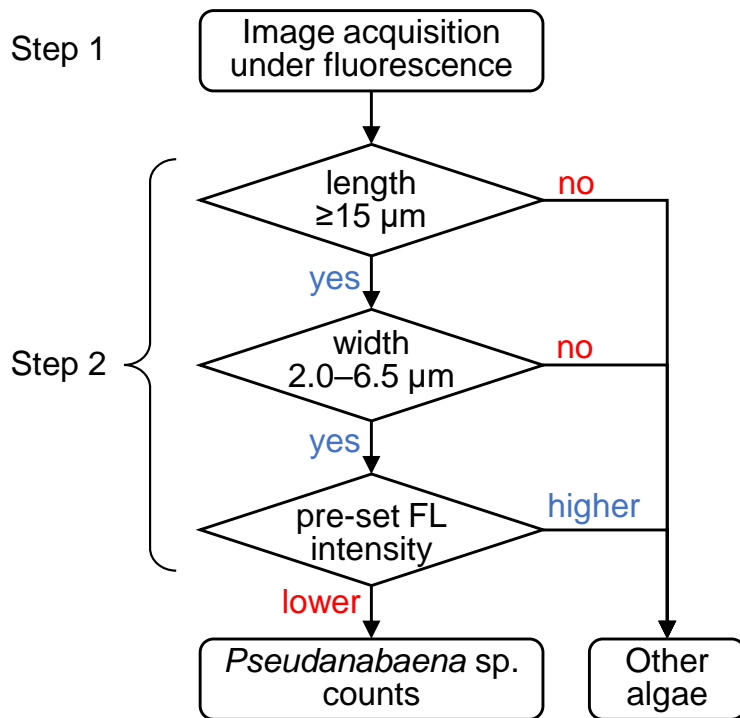


Fig. 4.5 Flowchart describing the developed automatic technique for determining *Pseudanabaena* sp. counts in lake water using the fluorescence (FL) microscopy and cell counting software.

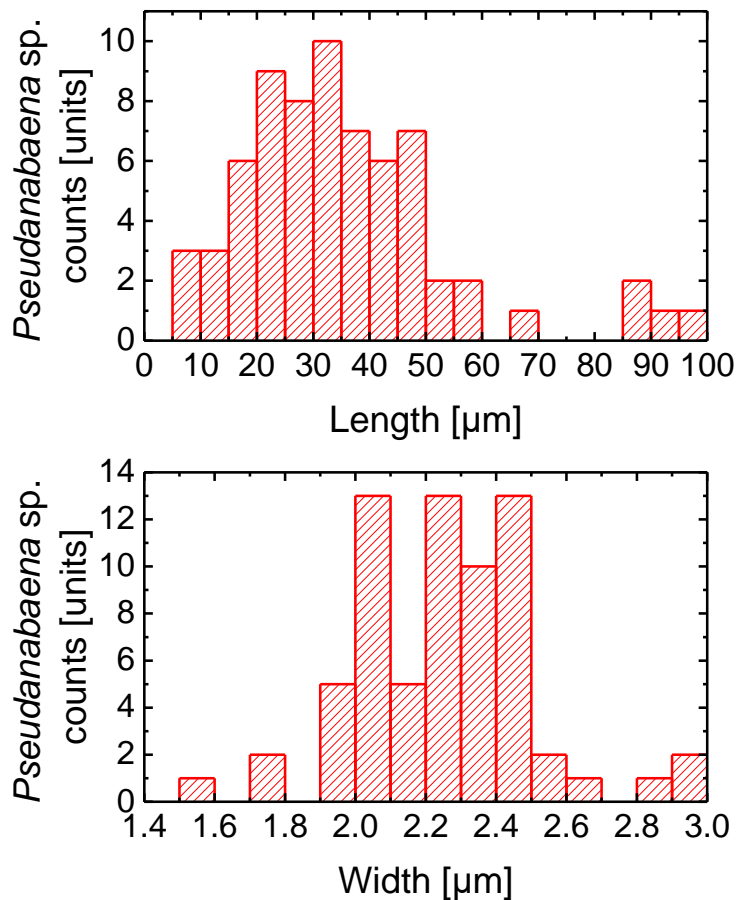


Fig 4.6 (a) Length and (b) width distribution of *Pseudanabaena* sp. in a pure culture sample that were captured in bright field ($n = 42$).

A major potential challenge of the developed method is the presence of short *Pseudanabaena* sp. composed of only 1–4 cells (a total length of $<15 \mu\text{m}$), which can lead to underestimation of the *Pseudanabaena* sp. count. This study conducted a preliminary analysis of 42 *Pseudanabaena* sp. units in a pure culture under bright-field observation mode, and showed that 15% of *Pseudanabaena* sp. ranged between $5 \mu\text{m}$ and $14 \mu\text{m}$ in length (**Fig. 4.6**). Although small *Pseudanabaena* sp. were rarely identified in natural lake water, particularly during the rapid increase phase in Lake Y, there is the chance that small *Pseudanabaena* sp. could dominate the *Pseudanabaena* sp. population depending on the lake or season. Further, the presence of filamentous cyanobacteria (e.g., *P. limnetica* or other

Pseudanabaena) or thin green algae (e.g. *Ankistrodesmus*) is another challenge. Their units can have a similar width to *Pseudanabaena* sp., which could lead to overestimation of *Pseudanabaena* sp. counts. These filamentous cyanobacteria represented a minority in Lake K in this study; thus, they did not influence the accuracy of the automated *Pseudanabaena* sp. counting method. Modifications of the developed auto-counting method may be required when cyanobacteria with similar dimensions to *Pseudanabaena* sp. form the majority of algae in a sample.

4.4. Validation of the developed method

Validation of the developed method was conducted using seven samples collected from Lake K (from two different points at four different sampling occasions). Prior to method validation, the counts of *Pseudanabaena* sp. and other algae were assessed in bright-field observation mode. At sampling point A, *Pseudanabaena* sp. counts under bright-field observation mode (i.e., manual counts) were 2,655 units/mL for the first sampling, progressively decreasing to 200 units/mL over the next three sampling occasions from September to November (**Fig. 4.7**). In contrast, *Pseudanabaena* sp. counts showed lesser variations at 343–928 units/mL at sampling point B. It is noted that total algae counts were more than one order of magnitude higher at $0.36\text{--}1.03 \times 10^5$ units/mL; these details are provided in **Table 4.3**. During the test, *Pseudanabaena* sp. represented small algal population at 0.3–4% (**Fig. 4.7**). Analyzing samples with a small percentage of the target algae is challenging for any auto-counting method because other algae can cause overestimation. Therefore, the seven samples used in this study can be considered a relatively difficult water matrix for auto-counting validation. The viability of the developed technique was assessed by manually or automatically counting algae in these seven samples. A high correlation was

observed between manually and automatically determined *Pseudanabaena* sp. counts in Lake K (Fig. 4.8).

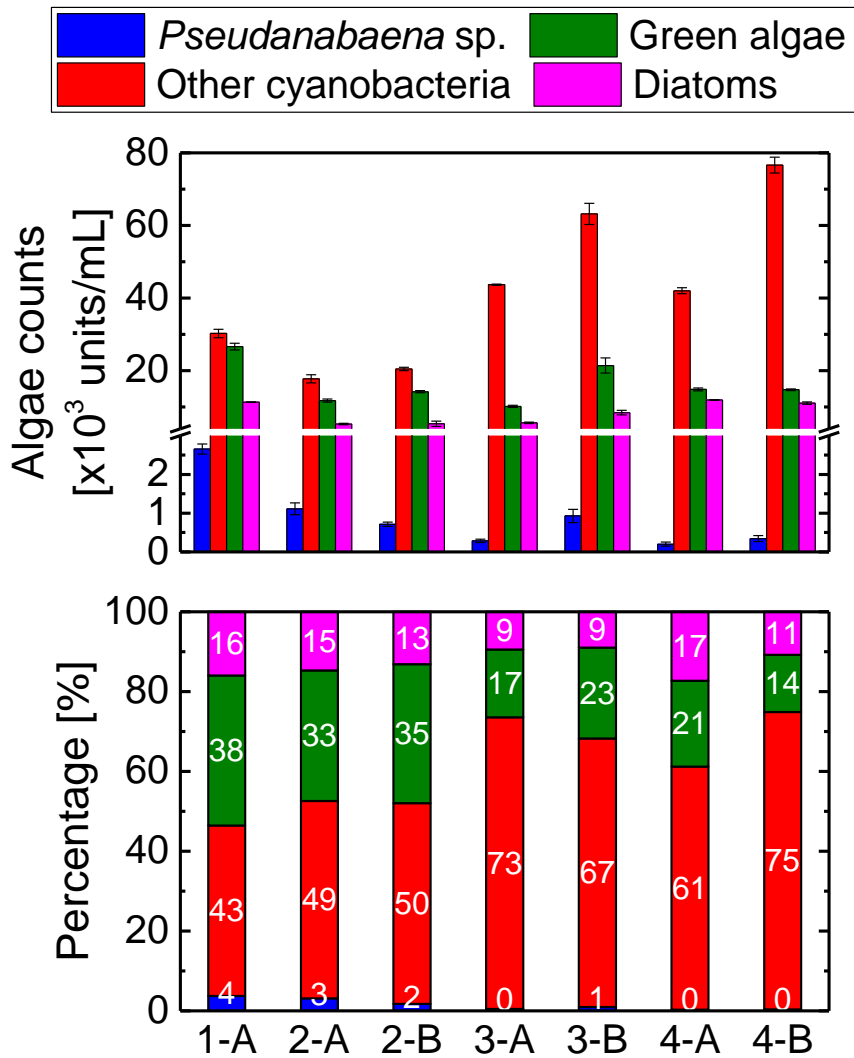


Fig. 4.7 Manually counted algae counts of Lake K in bright-field observation mode and their percentages. Samples were collected from two sampling points (A or B) on four different occasions (1–4) in 2020.

Table 4.3 Algae population (units/mL) in Lake K.

Date	29/09/ 2020	14/10/ 2020	14/10/ 2020	3/11/ 2020	3/11/ 2020	16/11/ 2020	16/11/ 2020
Sample	1-A	2-A	2-B	3-A	3-B	4-A	4-B
Cyanobacteria							
<i>Anabaeana</i>	0	0	0	0	0	0	0
<i>Anabaena affinis</i>	0	0	0	0	0	0	0
<i>Aphanocapsa</i>	3298	1242	471	2655	1927	4197	4112
<i>Merismopedia</i>	1028	1542	642	1713	4754	3683	4925
<i>Microcystis</i>	0	0	0	0	0	0	514
<i>Pseudanabaena</i> sp.	2827	771	728	385	899	300	557
<i>Pseudanabaena limnetica</i>	728	43	43	43	214	171	171
Others (unicellular or unidentified cyanobacteria)	25184	14904	19316	39275	57092	33965	67414
Diatoms							
<i>Cyclotella</i>	5696	2655	2570	2570	4069	5268	5354
<i>Aulacoseira granulata</i>	814	385	214	86	86	43	43
<i>A. granulata</i> var. <i>angustissima</i> f. <i>spiralis</i>	257	128	43	43	86	86	171
<i>Aulacoseira italica</i>	1842	600	514	343	43	514	600
<i>Synedra</i>	171	0	0	43	43	0	171
<i>Navicula</i>	557	43	257	171	685	171	171
<i>Nitzschia</i>	985	428	385	857	1499	1799	1328
Others	985	1028	1371	1542	1927	4026	3212
Green algae							
<i>Scenedesmus</i>	171	300	343	985	1199	985	1028
<i>Ankistrodesmus</i>	86	514	128	771	1242	1071	642
<i>Dictyosphaerium</i>	0	385	43	128	128	247	128
<i>Shroederia</i>	0	0	43	43	43	0	43
<i>Staurastum</i>	0	428	43	0	0	43	0
<i>Pediastrum</i>	0	86	0	0	0	0	43
Others	26340	10023	13577	8180	18546	12463	12892

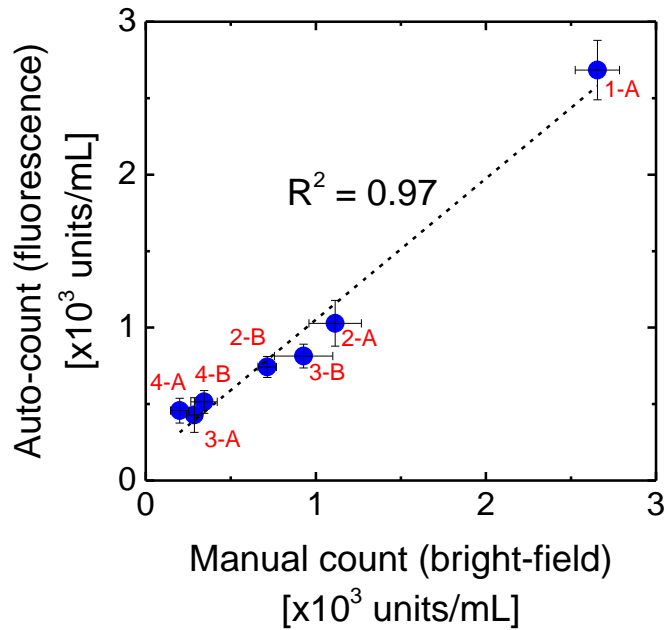


Fig. 4.8 Correlation between bright and fluorescent field counts in Lake K.

The auto-counting method generally overestimated the counts of *Pseudanabaena* sp., indicating that the developed method provides *Pseudanabaena* sp. counts with some errors. The cause of the miscounting was investigated by analyzing each image of the counted object in bright-field and fluorescence observation modes side-by-side. As a result, the major causes of the overestimation were as follows:

- Other cyanobacteria and green algae that have a similar length and width to *Pseudanabaena* sp.;
- Moving plankton (e.g., *Cryptomonas*, *Euglena*, or *Peridinium*) left trails of their paths during the image acquisition period, which became equivalent to *Pseudanabaena* sp. in size in the fluorescent images (**Fig 4.9**); and
- Double counting of long *Pseudanabaena* sp. in two different segmented images (**Fig. 4.10**).

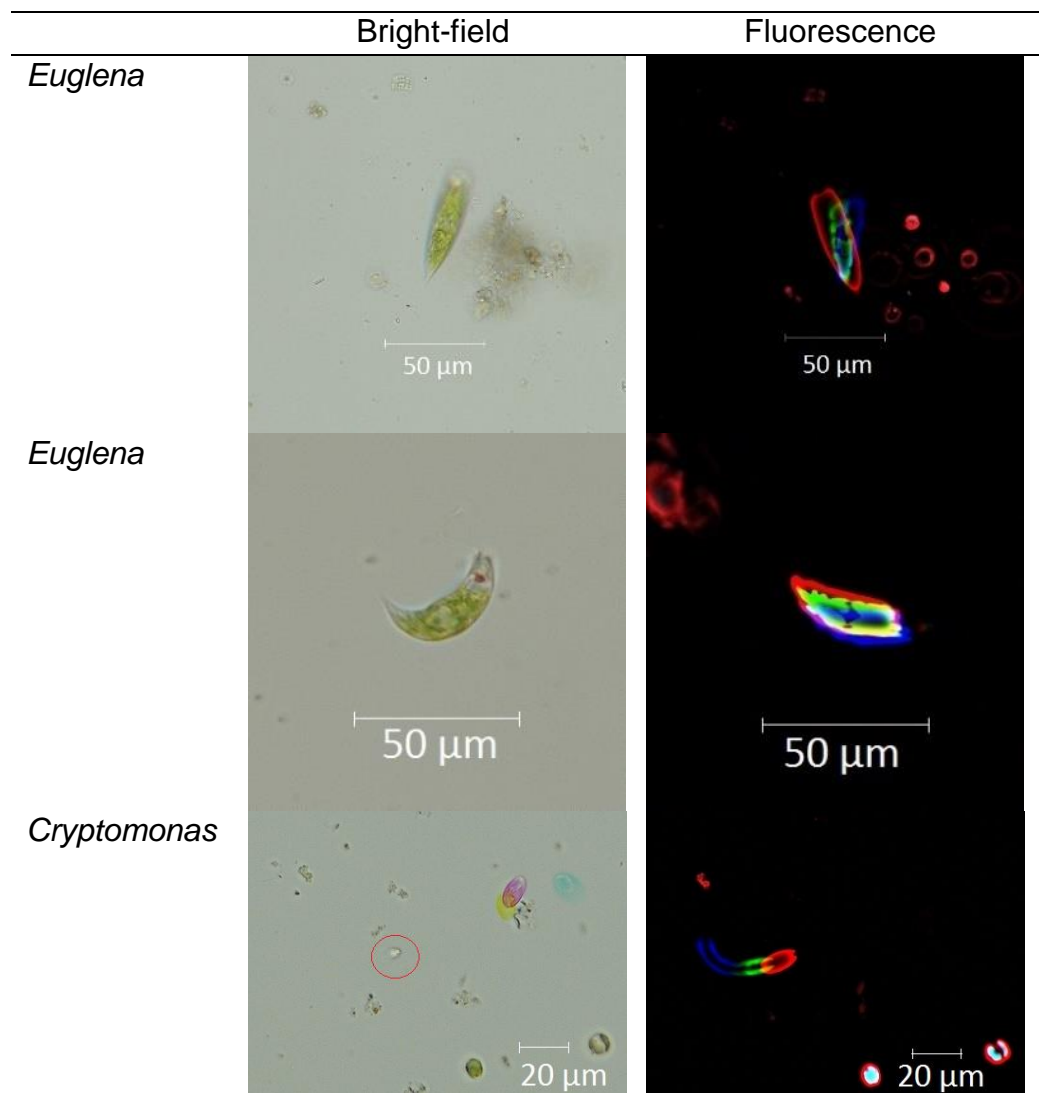


Fig 4.9 Microscopic images of *Euglena* and *Cryptomonas* in bright-field observation and the path of light created by moving plankton in fluorescence observation. They were not counted in bright-field observation.



Fig 4.10 A filament of *Pseudanabaena* sp. on two consecutive microscopic images in fluorescence observation: the single *Pseudanabaena* sp. was counted as two units with the developed auto-counting technique.

Table 4.4 Details of *Pseudanabaena* sp. counts, percentage of *Pseudanabaena* sp. in Lake K and error percentage between the manual and auto counts. The images analyzed represented a sample volume of 70 μ L.

Sample	1-A	2-A	2-B	3-A	3-B	4-A	4-B
Date	29/09/2020	14/10/2020	14/10/2020	3/11/2020	3/11/2020	16/11/2020	16/11/2020
Total algae count	4931	3089	3339	3542	6054	4733	6837
Manual counts of <i>Pseudanabaena</i> sp.	192	78	50	20	65	14	21
Auto counts of <i>Pseudanabaena</i> sp.	198	94	71	30	68	32	39
Percentage of <i>Pseudanabaena</i> sp. in the sample	3.9%	2.5%	1.5%	0.6%	1.1%	0.3%	0.3%
Error percentage	3.13%	20.51%	42.00%	50.00%	4.62%	128.57%	85.71%

Furthermore, the developed auto-counting method did not count some *Pseudanabaena* sp. due to their blurred (out-of-focus) appearance in the auto-captured images, resulting in an underestimation of *Pseudanabaena* sp. counts. The uncountability of some abnormal shaped algae in the images is a major drawback of image-based auto-

counting methods for filamentous algae, as reported in previous literature (Embleton et al., 2003; Hense et al., 2008). Overestimation of *Pseudanabaena* sp. counts was higher when the samples contained more green moving plankton and green algae such as *Ankistrodesmus* (**Table 4.3**). The error percentage increased when the percentage of *Pseudanabaena* sp. was below 0.5% at the end of Autumn (**Table 4.4**). The technique used in this study might not have the precision achieved by studies using algorithms or neuronal networks (Embleton et al., 2003; Coltelli et al. 2014), however the parameters used by the software can be easily adapted to suit the water source. Lake K is one of the most eutrophicated drinking water sources in Japan, it is not necessarily representative of *Pseudanabaena* sp. throughout Japan. Due to the potential for miscounting described above, the developed method cannot be treated as a tool for providing accurate counts of *Pseudanabaena* sp. in a similar way to conventional bright-field observations. However, it can be confidently concluded that the developed auto-counting method is a facile technique that can rapidly track changes in *Pseudanabaena* sp. counts in lake water with small *Pseudanabaena* sp. fractions among algae (0.5–4%).

4.5. Practical applications

The facile auto-counting technique for *Pseudanabaena* sp. counts enables site workers without algal analysis skills to frequently assess *Pseudanabaena* sp. counts. *Pseudanabaena* sp. counts can be a surrogate indicator of 2-MIB occurrence; thus, frequent analysis using this technique can trigger early warnings to drinking WTPs to address upcoming 2-MIB peaks in cyanobacterial blooms and can assist plant operators in making decisions on adjusting the dose of PAC or ozone. Further, the developed technique can assess the outcome of *Pseudanabaena* sp. throughout the water treatment processes.

Although the developed auto-counting method has the potential to overestimate *Pseudanabaena* sp. counts, a perfect match with no errors is not a priority when algae counts are used as a surrogate indicator of odor occurrence. Nonetheless, the degree of overestimation and underestimation can vary depending on the dimensions (e.g., length and width) of *Pseudanabaena* sp., which could be location specific. Although Lake K is one of the most eutrophicated drinking water sources in Japan, it is not necessarily representative of *Pseudanabaena* sp. throughout Japan. Moreover, some *Pseudanabaena* taxa that do not produce 2-MIB (Shizuka et al., 2020) can be counted as “*Pseudanabaena* sp.” due to their similarity in size. Therefore, to identify the validity of the developed dimensional criteria and requirements for criteria adjustments, further validation using different drinking water sources will be conducted in a future study.

A limitation of this study is that the detection of high odor occurrence through automated counting of *Pseudanabaena* sp. was not assessed due to a lack of odor occurrence in Lake Y throughout the summer in 2020 and the limited accessibility of odor-occurring samples in autumn. The occurrence of 2-MIB is typically identified during the growth phase of *Pseudanabaena* sp. in summer rather than its death phase in autumn. Therefore, further validation of frequent *Pseudanabaena* sp. auto-counting to track 2-MIB occurrence will be conducted in a future study.

Chapter 5 Online monitoring of bacteria

5.1. Online bacterial counts and pre-treatment performance

5.1.1. Bacterial counts in the rapid sand filter effluent

Real-time bacteriological counter coupled with the dialysis membrane-based pre-treatment system provided a continuous profile of bacterial counts in the sand filter effluent for the 19-d test. Online bacterial counts in the sand filter effluent varied considerably, between 0.2×10^4 and 2.5×10^4 counts/mL (**Fig. 5.1a**). During the first day, bacterial counts gradually decreased from 0.9 to 0.1×10^4 counts/mL. The peak, up to 1.5×10^4 bacterial counts/mL, appeared immediately after backwashing on day two. Thereafter, bacterial counts in the sand filter effluent progressively decreased to 0.2×10^4 counts/mL and remained relatively stable until the following backwashing on day five. Similar bacterial count variations were observed every 3-d filtration cycle (3-d filtration and backwashing of the sand filter). However, the impact of backwashing on bacterial counts varied every backwashing, showing the highest peak at 2.5×10^4 counts/mL (second day) and the lowest peak at 0.8×10^4 counts/mL (eighth day). Except for several hours after backwashing, online bacterial counts in the sand filter effluent were observed below 1.0×10^4 counts/mL during the test period. The bacterial concentrations under a steady-state condition (e.g., below 1.0×10^4 counts/mL) can be utilized as a baseline for generating a warning of filtration failures or filter malfunctions.

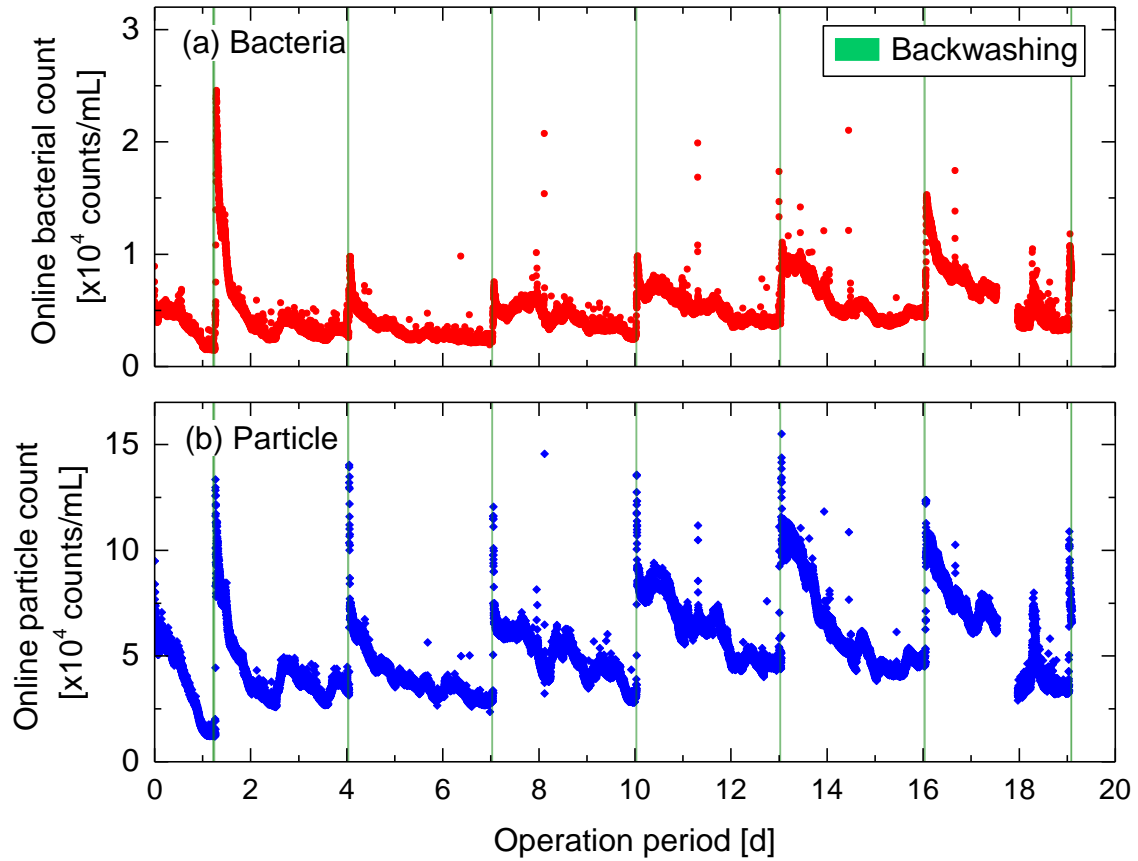


Fig. 5.1 Online (a) bacterial counts and (b) particle counts in the sand filter effluent. Each point represents the counts measured during 1 min. Points represent measurements for every 1 min. The real-time bacteriological counter halted for 8 h on the 18th day due to a problem in a sampling pipe detached from the effluent sampling point.

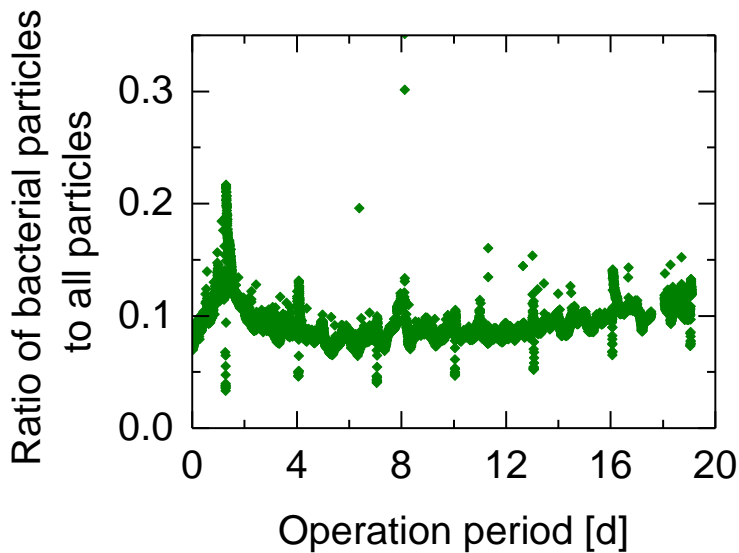


Fig. 5.2 Ratio of bacterial counts to particle counts in the filtrate.

Particle counts with $\geq 0.5 \mu\text{m}$, which were monitored through the detection of scattered light for each particle, were also recorded for comparison with the bacterial particles. The particle counts ($1\text{--}15 \times 10^4$ counts/mL) (**Fig. 5.1b**) were generally one order of magnitude higher than bacterial counts (**Fig. 5.2**). Particle counts also showed a similar trend as bacterial counts; particle counts reached a peak after each backwashing and decreased over filtration time during a 3-d filtration cycle. The trend of decreasing particle counts over filtration time was typically found in the sand filter effluent (Colton et al., 1996; Soyer et al., 2013). The removal of particles in the sand filter occurs through their attachments onto the sand; they are captured through diffusion, gravity, hydrodynamic forces, straining, or interception mechanism (Cescon and Jiang, 2020; Ives, 1970). Over time, the pore of sand filter (empty space among the sand particles) with a diameter of approximately $100 \mu\text{m}$, which depends on the diameter of sand filter media, can be reduced with the attached particles, resulting in improved efficiency of the filter for particle removal despite the increased hydraulic resistance. Therefore, it can be presumed that during the backwashing process the sands in the filter were cleaned from the attached particles and bacteria. Therefore, after backwashing,

the sand pores returned to the original pore size (e.g., 100 µm diameter), allowing more particles and bacteria to pass through the filter. Overall, the results indicate that changes in bacterial and particle counts during sand filtration can occur simultaneously.

It is noted that short peaks during the steady-state filtration during the filtration cycle between backwashing steps occurred in bacterial counts at 8, 11, 13, 14, and 16 d (**Fig. 5.1**). These peaks were very brief events lasting <5 min. The short and sudden peak possibly occurred according to the disintegration of some biofilm from the full-scale sand filter iron-cast pipe or PTFE sampling tubes connecting between the full-scale sand filter pipe and the real-time bacteriological counter. Release of bacteria from pipes can occur due to the variation in flow velocity and nutrient supply;(Chan et al., 2019; Sawyer and Hermanowicz, 1998; Tsai, 2005) thus, the short peaks do not necessarily indicate that the sand filter efficiency for bacterial removal was compromised. It can be suggested that only peaks that last longer than longer periods (e.g., 10 min) may be considered to be a filter malfunction. However, to avoid false alarms, the pipes between the sampling point and real-time bacteriological counter (PTFE tube this time) may require periodical changes or cleaning.

5.1.2. The fate of bacteria before and after backwashing

The variations in bacterial and particle counts at backwashing were evaluated in detail to provide an understanding of bacterial fates before and after backwashing. At the beginning of each backwashing, the effluent valve of the full-scale sand filter was closed, and no water from the sand filter basin was drawn to the effluent pipe. Because the instrument was analyzing a residual sand filter effluent remaining in the effluent pipe, both bacterial and particle counts remained low at $0.3\text{--}0.5\times 10^4$ counts/mL during 30–40 min (**Fig. 5.3**). After re-starting filtration, the water in the effluent pipe was presumably replaced with the newly filtered water, and particle counts showed a peak at 35–55 min. Studies have reported an

increase in residual particle counts and manually analyzed bacterial counts following backwashing (Ahmad et al., 1998; Colton et al., 1996). This indicates that the high peak in particle counts (or turbidity) typically happens soon after backwashing.

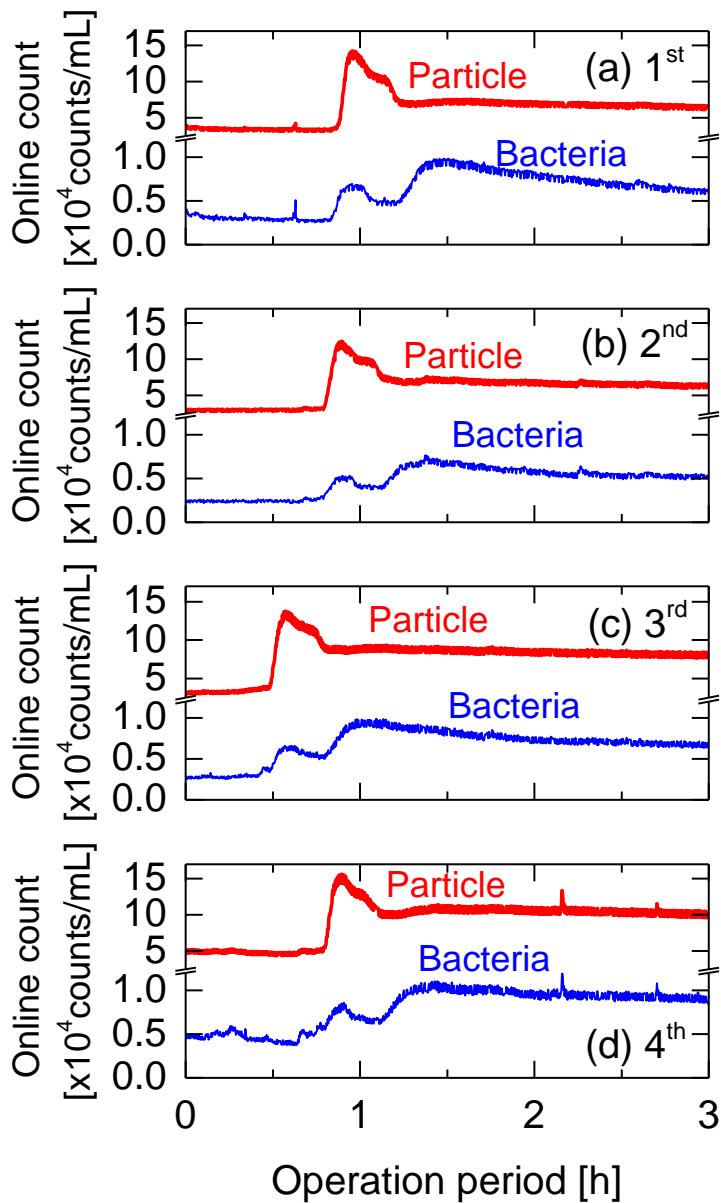


Fig. 5.3 Online counts of particles (red) and bacterial particles (blue) in the 3rd filter effluent during backwashing process starting at 9:00 am at the operation period of 5th (a), 8th (b), 11th (c), and 14th day (d). Lines are made based on every 6 s data. Following each backwashing process, the filtration of sand filter resumed at 0 h.

Similar to particle counts, bacterial counts showed a peak at 35–55 min. However, another peak at higher counts appeared at 1.0–1.5 h; then bacterial counts gradually decreased, which did not correspond to the peak or variation in particle counts during the same period. Therefore, the ratio between bacterial counts to particle counts varied considerably soon after each backwashing step (**Fig. 5.2**). The results indicated that the peak of bacterial counts occurred after that of particle counts. Furthermore, the variations in bacterial counts are unlikely detected with typical particle counters due to the difference in their counts with one order of magnitude. Because bacterial information is more relevant to biological water quality than particle information, the results indicated an advantage of monitoring bacterial counts online along with conventional particle counts.

5.1.3. Stability of pre-treatment

The stability of dialysis membrane-based pre-treatment during the long-term operation was assessed to identify its feasibility for long-term operation. The real-time bacteriological counter utilizes light with an Ex wavelength of 405 nm, and the detectors measure the intensity of fluorescence light at 415–450 (Band A) and 490–530 nm (Band B), respectively. However, because of the dissolved interfering substances, there was a strong background fluorescence even in the sand filter effluent. It is noteworthy that when the sand filter effluent was monitored without the pre-treatment system, the real-time bacteriological counter displayed an error message of exceeding the capacity of fluorescence light detectors, which disabled direct analysis of sand filter effluent.

In general, the pre-treatment system stably attenuated the concentrations of background interfering substances despite the daily variations in the raw water sources and sand filter flow rate (**Fig. 5.4**). The normalized background fluorescence intensity of 1.0 (**Fig. 5.4c**) is the maximum level measurable by the real-time bacteriological counter. Normalized

fluorescence intensity of the real-time bacteriological counter started at approximately 0.15, which indicated 15% level of the counter's fluorescence light detectors capacity. The background interfering substances, transferred from the sample solution (i.e., sand filter effluent) to the dialysate, seemed stably attenuated by anion exchange resins in the dialysate line, therefore the accumulation of these substances in the dialysate was prevented. However, normalized fluorescence light intensity slightly varied every day according to the variation in intake flow rate. The changes in the intake water flow rate at this plant altered the retention time in the coagulation, flocculation, and sedimentation basins due to the specific basin capacities, whereas coagulant doses were maintained constant for varied flow rates. Similar to turbidity, changes in treatment time can modify the growth of floc with humic acids, which ultimately lead to changes in their removal (Wei et al., 2009; Wu et al., 2019). Therefore, the removal of background interfering substances by these full-scale treatment processes also varied, and it affected their residuals after the dialysis-based pre-treatment system. Thus, the background interfering substances accumulated in the AER resins, resulting in a gradual increase in the normalized fluorescence light intensity of the pre-treated sand filter effluent. Despite the daily variations and gradual increases, the normalized fluorescence light intensity remained below 1.0 throughout the 19-d test, indicating the pre-treatment could last longer than 19 d.

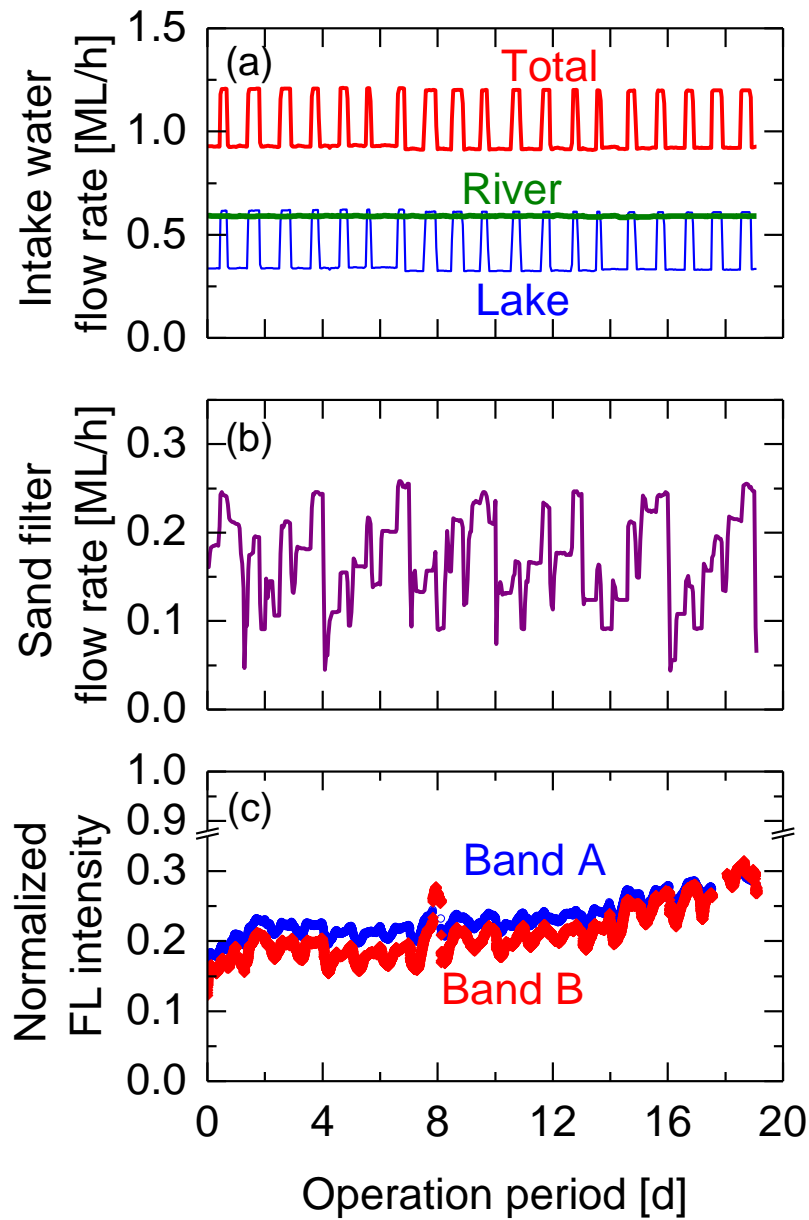
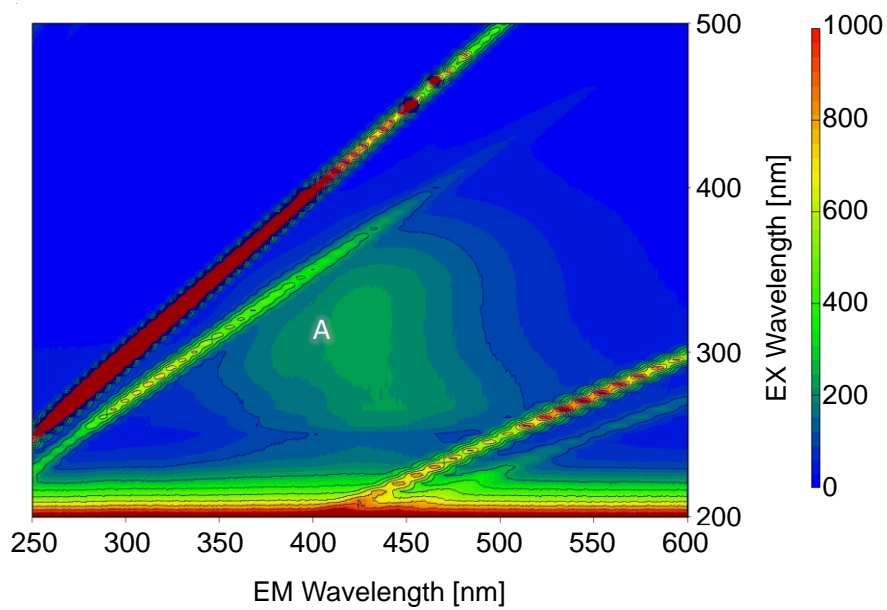
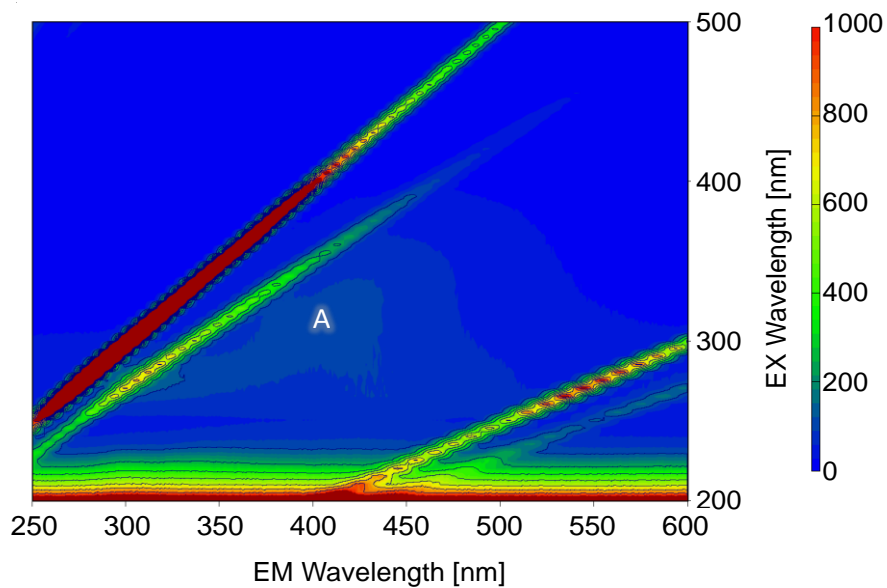


Fig. 5.4 (a) Flow rate of raw water intake, (b) #3 sand filter flow rate, and (c) background fluorescence (FL) intensities of bands A and B for the pre-treated sand filter effluent prior to the real-time bacteriological counter.

The untreated and pre-treated sand filter effluents were further characterized by performing an excitation emission matrix spectrum to identify the source of the interfering substances remaining in the pre-treated sand filter effluent after the 19-d test. The sand filter effluent showed high fluorescence intensities at the peak excitation and emission wavelengths of 315 and 425 nm (**Fig. 5.5a**). The peak region in the surface waters indicated the presence of humic acids (Chen et al., 2003; Nam and Amy, 2008). The level of interference in the measurement of the real-time bacteriological counter in bands A and B could be confirmed when it was assessed at the excitation wavelength of 405 nm (**Fig. 5.6**). After the pre-treatment, the peak intensities of the pre-treated sand filter effluent in region A decreased (**Fig. 5.5b**). Similarly, the fluorescence intensities of the pre-treated sand filter effluent in bands A and B decreased (**Fig. 5.6**), indicating that the dialysis membrane-based pre-treatment system successfully attenuates the concentrations of background interfering substances after the 19-d test. Overall, the pre-treatment system could be stably operated without replacement of dialysis membranes and anion exchange resins over one month, which is a feasible replacement period of consumables for online instruments.



(a) Before pre-treatment



(b) After pre-treatment

Fig. 5.5 Excitation emission matrix spectra of the 3rd filter effluent collected at 19th day.

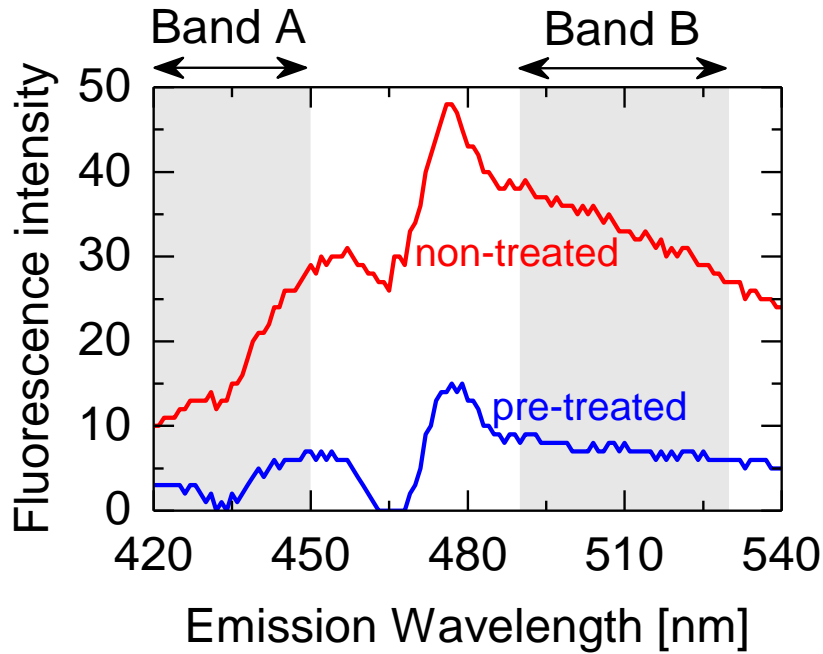


Fig. 5.6 Fluorescence intensity at an excitation wavelength of 405 nm in the non-treated (red) and pre-treated (blue) sand filter effluent collected on the 19th day. The spectra of each sample were obtained by subtracting the fluorescence spectrum of water.

5.2. Bacteria in the rapid sand filter effluent

5.2.1. Assessment of bacterial community

The bacterial community of the sand filter effluent was assessed on two sampling occasions. The objective was not a comparative study of the microbial community dynamics but obtaining information about the type of bacteria monitored by the real-time bacterial counter. Among the bacteria phylum, Proteobacteria, Planctomycetes, and Cyanobacteria were dominant, accounting for more than 75% (**Fig. 5.7**). Proteobacteria has been reported as the major bacterial community of filter effluent in previous studies (Liu et al., 2018; Park et al., 2016; Potgieter et al., 2018). The main class of Proteobacteria was Alphaproteobacteria (45.5% and 59.5% on days 5 and 12, respectively), which mainly comprised the family *Methylobacteriaceae* (**Fig. 5.8**). Similarly, other Proteobacteria classes were dominated by

specific families: Betaproteobacteria comprised of *Comamonadaceae* and *Oxalobacteraceae*, and Gammaproteobacteria comprised of *Enterobacteriaceae* and *Pseudomonadaceae*. This study identified a negligible portion of Deltaproteobacteria (<1%), which is similar to a previous study (<1%)(Park et al., 2016) but different from another study (approximately 15%) (El-Chakhtoura et al., 2015).

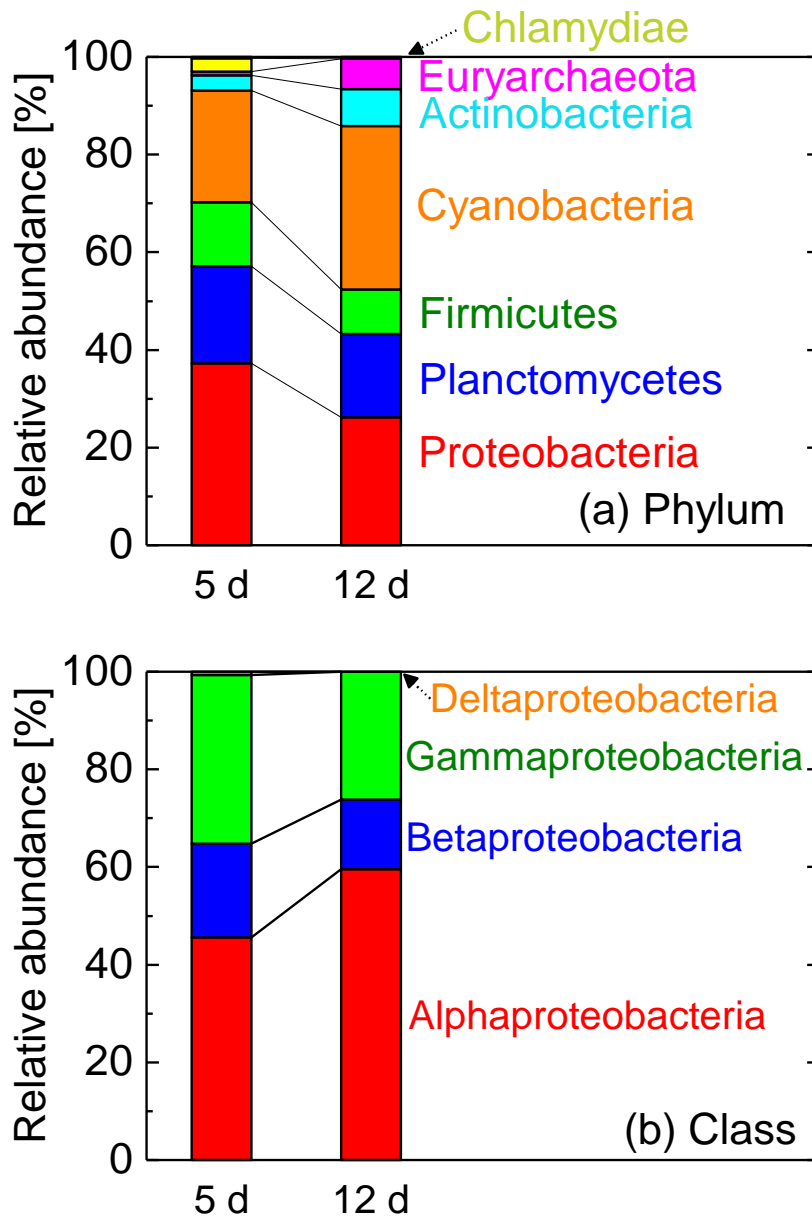


Fig. 5.7 Relative abundance of bacteria in the sand filter effluent samples collected at days 5 and 12: (a) Phylum and (b) Class among Proteobacteria.

Apart from Proteobacteria, this study found that the dominant family among Planctomycetes was different in the two samples. The main family was *Planctomycetaceae* on day 5 and *Isosphaeraceae* from the *Gemmatales* order on day 12 (**Figs. 5.8 and 5.9**). On day 5, *Planctomycetaceae* accounted for 18.4% of total OTUs, and only 0.3% of total OTUs was found on day 12. *Isosphaeraceae* were not present on day 5, but they accounted for 12.7% of total OTUs on day 12. The details for the families of Cyanobacteria were not identified. Despite the variation in bacterial communities in the sand filter effluent between two sampling occasions and other studies, bacterial communities found in this study can be considered as typical for a sand filter effluent.

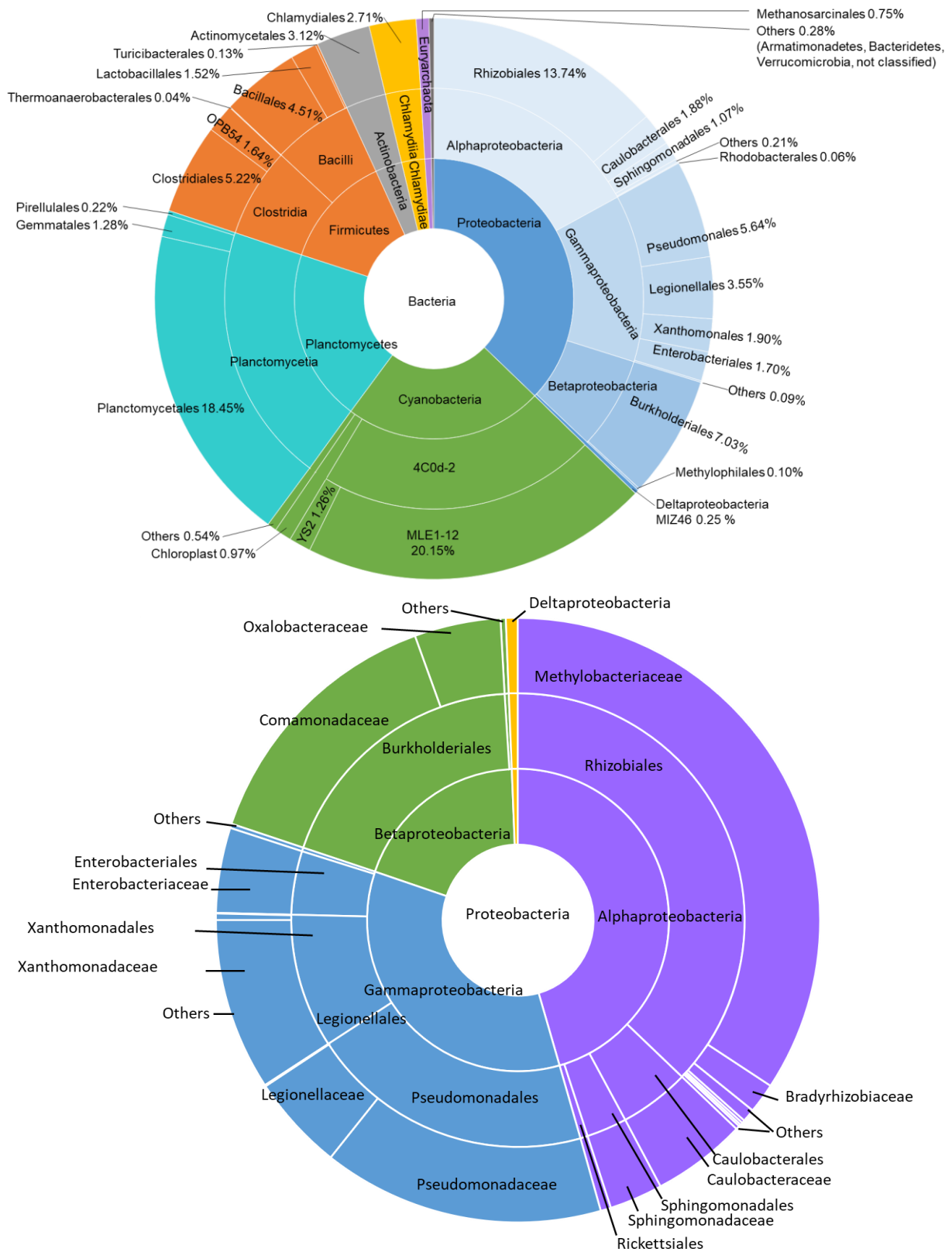


Fig. 5.8 Bacterial communities of the sand filter effluent collected at 5th d.

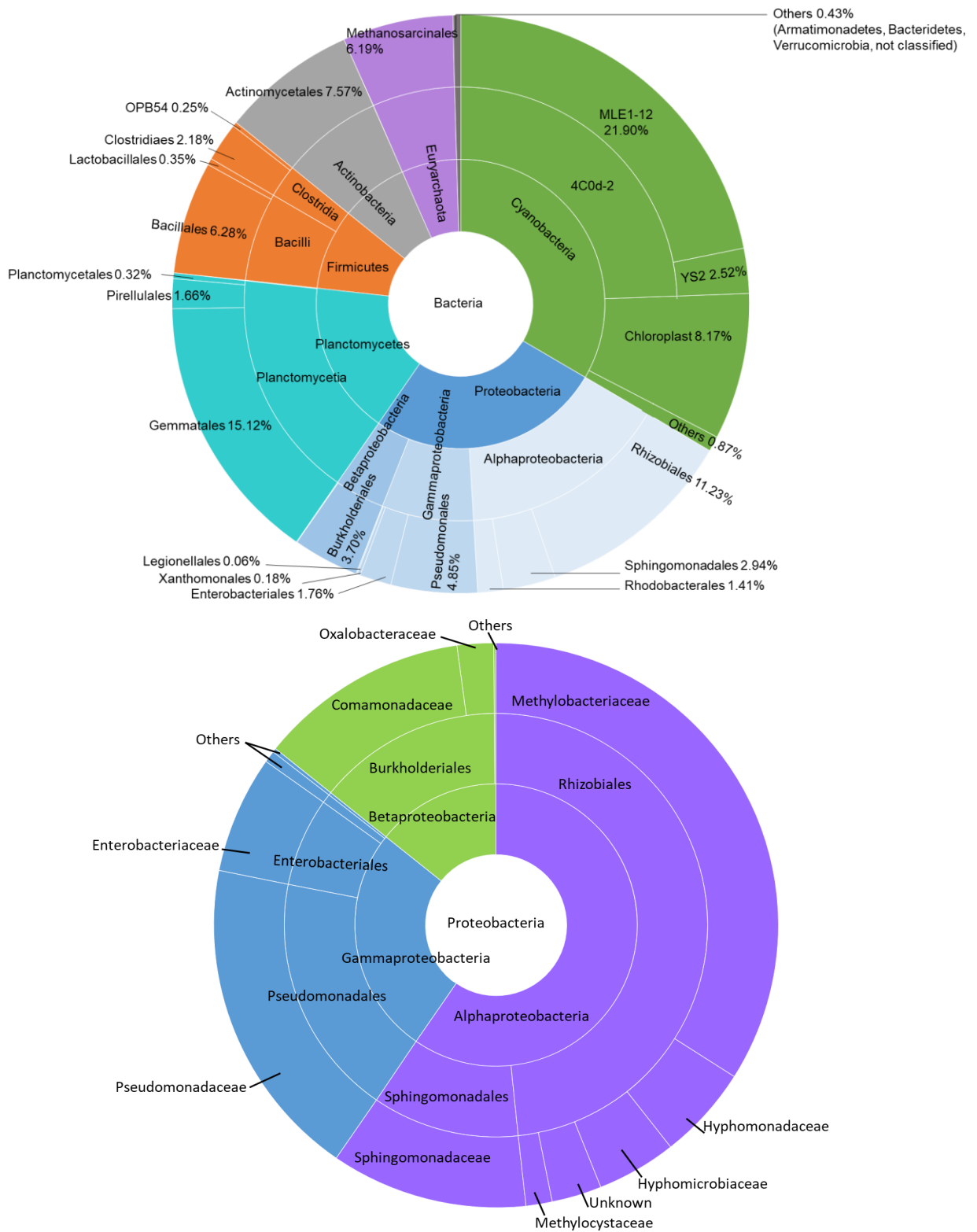


Fig. 5.9 Bacterial communities of the sand filter effluent collected at 12th d.

5.2.2. Assessment of the bacterial quantity

The validity of online-monitored bacterial counts in the rapid sand filter effluent was evaluated by comparing with bacterial counts manually analyzed through conventional bacteria counting techniques. Microscopic total bacterial counts obtained using a stain (SYBR® green I, SYTO™ 9, or AO) that provides total bacterial counts (i.e., a total of non-damaged and damaged bacterial cells) were generally over one order of magnitude higher than the online-monitored bacterial counts (**Fig. 5.10**). The total bacterial counts ranged from 0.7×10^5 to 3.0×10^5 , which were similar to that in previous studies ($1.0\text{--}5.0 \times 10^5$ counts/mL, respectively)(Nescerecka et al., 2018; Park et al., 2016) that utilized a similar rapid sand filter system.

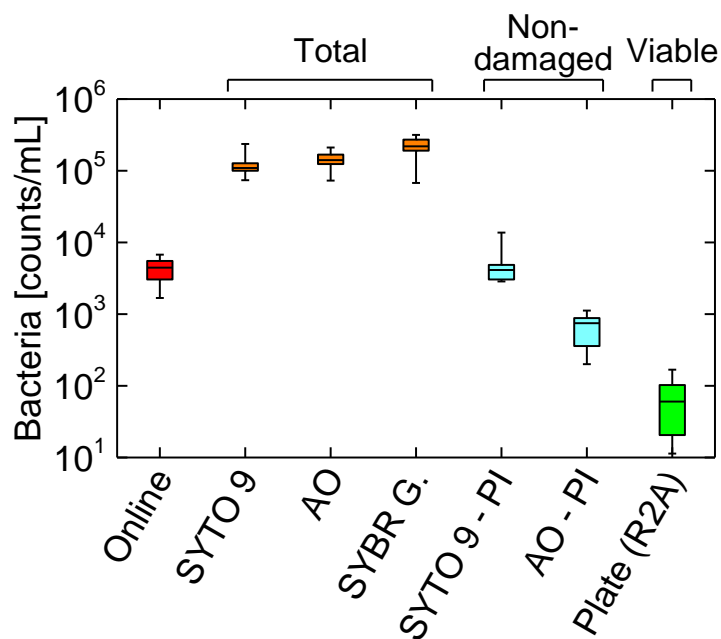


Fig. 5.10 Online bacterial and manual bacterial counts: Lower and upper box boundaries represent 25th and 75th percentiles, respectively, line inside box represents median, and lower and upper error lines represent maximum and minimum counts, respectively. Samples were collected at the 2nd, 4th, 5th, 8th, 9th, 12th, 15th, and 19th day.

Among the three stains of total bacterial counts, SYBR[®] Green I showed a strong correlation with online bacterial counts ($R^2 = 0.90$) (**Fig. 5.11a**). Bacteria stained with the other stains (i.e., SYTO[™] 9 and AO) showed minor correlations ($R^2 = 0.68$ and 0.39 , respectively). The differences in total bacterial counts could be explained by differences in binding specificities or membrane permeability of the different dyes. For example, the permeability of bacterial cell membrane for SYTO[™] 9 stains can vary depending on bacterial types such as gram-positive and gram-negative bacteria (McGoverin et al., 2020; Stiefel et al., 2015), which could occur to other stains. Although the variations in their total bacterial counts cannot be fully explained by their staining mechanisms, AO and SYTO[™] 9 overlook some bacteria in the environment water. In fact, most previous studies determining bacterial counts during drinking water treatment have used SYBR[®] green I (Phe et al., 2005; Ramseier et al., 2011). This supports the applicability of SYBR[®] green I for evaluating bacterial counts in drinking water. However, total bacterial counts were much greater than online-monitored bacterial counts.

To explore potential indicators of bacterial counts relevant to online-monitored bacterial counts, the relevance of non-damaged bacterial counts was also assessed. Although the counts of non-damaged bacteria stained with SYTO[™] 9 + PI were found at the same order of magnitude as online bacterial counts (**Fig. 5.10**), low correlations between online-monitored bacterial counts and non-damaged bacteria stained with SYTO[™] 9 + PI or AO + PI were obtained (**Fig. 5.11b**). It should be noted that bacterial counting with SYBR[®] Green I + PI was not conducted in this study. The ratio of non-damaged bacterial counts to total bacterial counts was below 10%, indicating that most of the bacteria in the sand filter effluent was damaged. The ratio of damaged bacteria was stable throughout the experiment. The low ratio (i.e., a large proportion of damaged bacteria) could have occurred due to intermediate chlorination performed prior to the sand filter basins for mitigating algal and bacterial growth

in the sand filter basin. In fact, chlorination can cause sublethal damage to the membrane preceding cell death in gram-positive cells (Virto et al., 2005). The standard plate counts showed a wide range from 11 to 169 CFU/mL, thus their counts were lower than the online-monitored counts and no correlation was found (**Fig. 5.11c**).

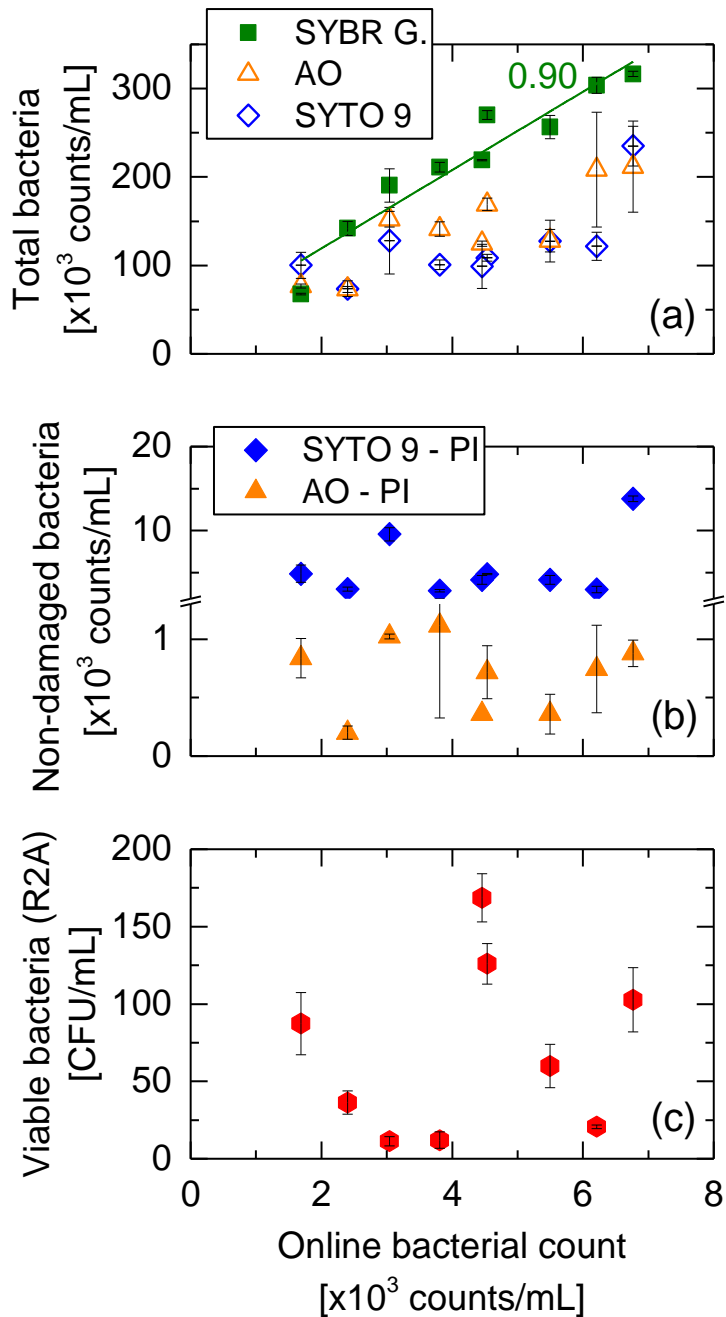


Fig. 5.11 Correlation between manual bacterial (a, b and c) and online bacterial counts:

Samples were collected at the 2nd, 4th, 5th, 8th, 9th, 12th, 15th, and 19th day.

This study found that non-damaged bacterial cells determined using stains can be irrelevant to those counted by the real-time bacteriological counter. Their low correlation may be due to the fundamental difference in analysis mechanisms (**Fig. 5.12**). The real-time bacteriological counter measures the intensity of auto-fluorescence light emitted from the riboflavin and NADH of each bacterium (**Fig. 5.13**), which are presumably not affected by the state of cell membranes. Therefore, some of the bacterial cells with damaged membranes might have been counted as online-monitored bacterial counts, which can cause discrepancies in numbers between non-damaged bacterial counts and online-monitored bacterial counts. Moreover, the real-time bacteriological counter excludes bacterial particles smaller than 0.5 μm , which can be counted by staining followed by fluorescence microscopy. Despite the differences in the magnitude of bacterial counts, the total bacterial counts obtained with SYBR[®] Green I staining, which has been accepted as a parameter of presenting bacterial contaminations in the research of drinking water, can be utilized as an indicator of online-monitored bacterial counts. Therefore, as an alternative of the time-consuming cell staining method, the real-time microbiological counter can provide an early warning of filter malfunctions or potential contaminations in the sand filter effluent.

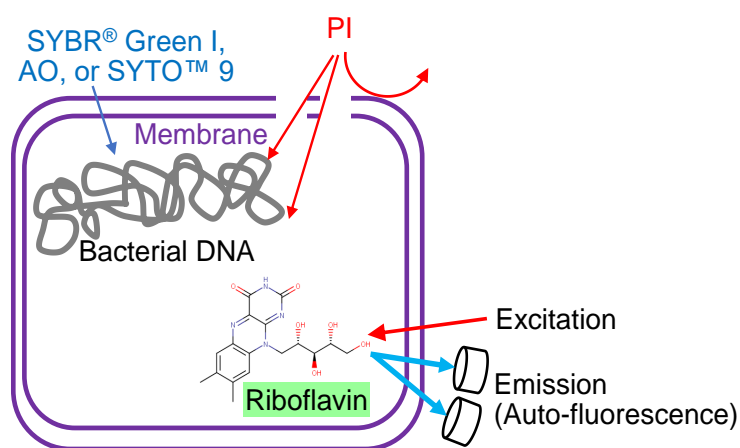
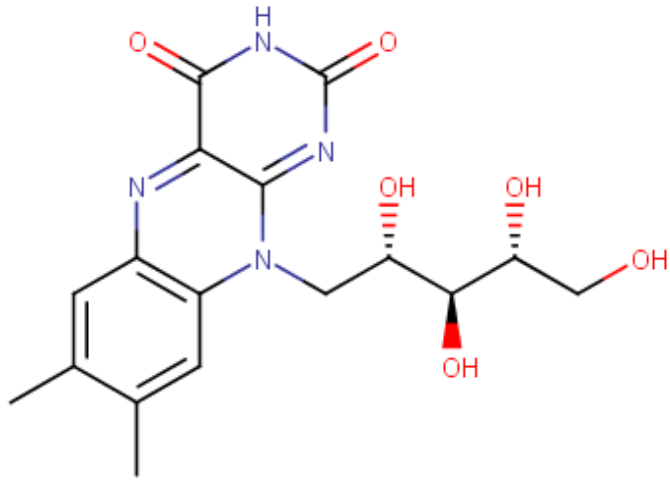
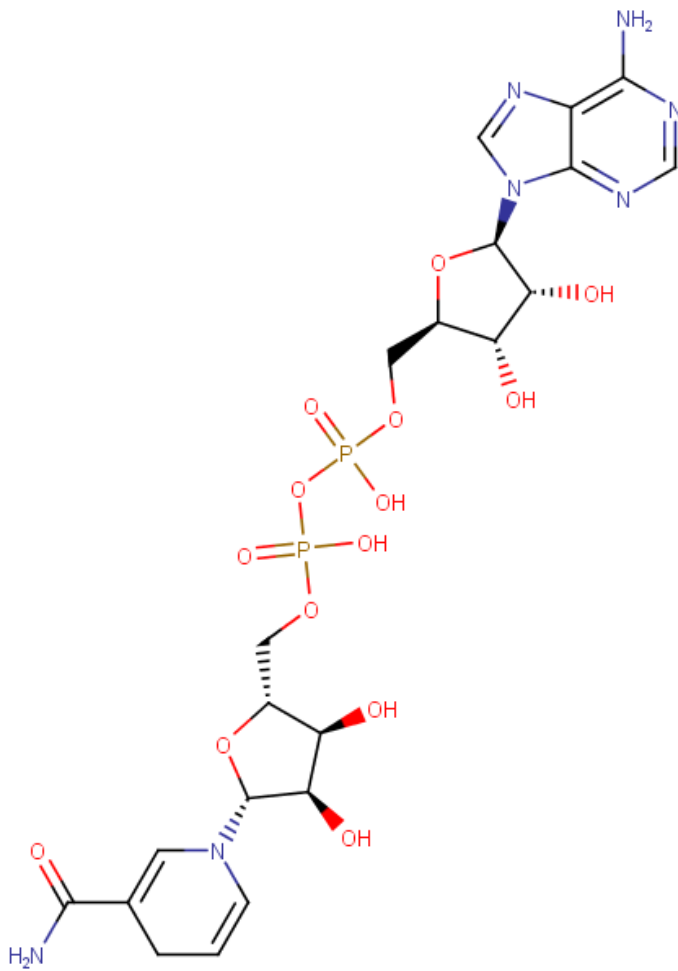


Fig. 5.12 Components of bacterial cells that are relevant to stains and real-time bacteriological counter: PI = propidium iodide and AO = acridine orange.



(a)



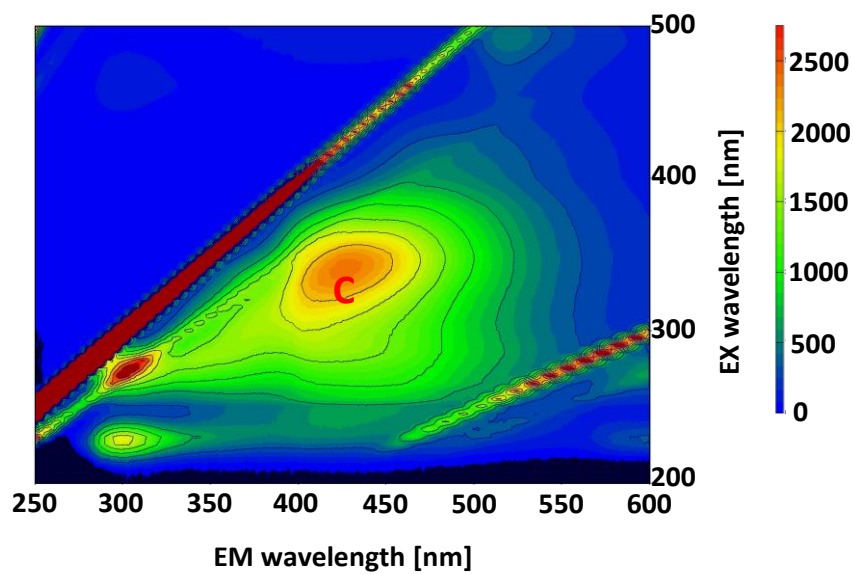
(b)

Fig. 5.13 Chemical structure of (a) riboflavin and (b) NADH.

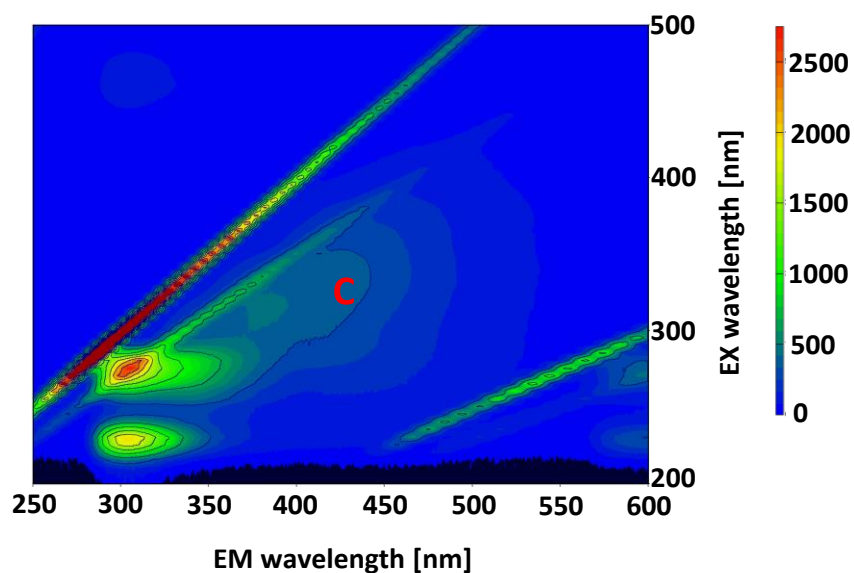
Chapter 6 Online monitoring of bromate

6.1. Importance of the NF pre-treatment system

The inconclusive direct online analysis of bromate ions in the MBR-treated wastewater samples could be attributed to the high concentrations of interfering substances that emitted auto-fluorescence at EX300/EM400, which exceeded the detection limit of the online analyzer. The major sources of the interference at these wavelengths were humic acid-like fluorophores, with EX/EM of 320–360 nm/400–450 nm (denoted as peak C) (**Fig. 6.1a**) (Carstea et al., 2016). The intensity of humic acid-like fluorophores can be considerably reduced by conducting NF pre-treatment (**Fig. 6.1b**). NF pre-treatment can remove many interfering substances in the MBR-treated wastewater because the NF270 membrane has an MWCO of approximately 300 Da, and humic substances, including humic acids and humic acid-like substances, have molecular weights > 350 Da (Huber et al., 2011; Yoon, 2019).



(a) Feed



(b) Permeate

Fig. 6.1 Excitation and emission spectra of membrane bioreactor effluent: (a) before and (b) after NF pre-treatment. The data was attained during NF pre-treatment at a feed temperature of 35 °C and a permeate flux of 1 L/m²h.

6.2. Optimization of pre-treatment conditions

The permeate flux and feed temperature during the NF pre-treatment were optimized by assessing the permeation of bromate ions and interfering substances, indicated by the fluorescence intensities EX300/EM400, in the MBR-treated wastewater. A permeate flux of $1.0 \text{ L/m}^2 \text{ h}$ at a feed temperature of $35 \text{ }^\circ\text{C}$ helped achieve 99% permeation of bromate ions (that is, almost no bromate ions were removed) and 28% permeation of the interfering substances (that is, 72% of the interfering substances were removed) (**Fig. 6.2a**). No errors were observed with the use of the online bromate ion analyzer, and this was attributable to the NF-treated wastewater, indicating an adequate removal of the interfering substances. A permeate flux $< 1.0 \text{ L/m}^2 \text{ h}$ could not be achieved because of the friction loss in the NF pre-treatment system to maintain a cross-flow rate of 700 mL/min . Although increasing the permeate flux to $5 \text{ L/m}^2 \text{ h}$ decreased the permeation of the interfering substances up to 21%, bromate ion permeation also decreased (89%), suggesting that 11% of the bromate ions were rejected by the NF membrane. The changes in solute permeation occur owing to the changes in solute and solution permeation; solute permeation through membranes is less affected by changes in the permeate flux (Wijmans and Baker, 1995).

Furthermore, increased feed temperatures affected the permeation of both bromate ions and interfering substances. An increase in feed temperature from $20 \text{ }^\circ\text{C}$ to $35 \text{ }^\circ\text{C}$ resulted in an increase in the permeation of interfering substances from 21% to 28%, while increasing the permeation of bromate ions from 94% to 99% (**Fig. 6.2b**). The changes in solute permeation are affected by temperature variations because of the changes in the membrane pore size and the permeability of solutes; at high temperatures, the pore size of the NF membrane and the permeability coefficient of solutes increase. (Sharma et al., 2003) (Tsuru et al., 2010) The permeation of bromate ions and interfering substances revealed a similar increasing trend based on the changes in permeate flux and feed temperature (**Fig. 6.3**). Thus,

complete separation of bromate ions from the interfering substances using the NF270 membrane was impossible. As the minimum removal of bromate ions by the NF membrane is a preferred pre-treatment approach, the lowest permeate flux (1.0 L/m²h) and the highest feed temperature (35 °C) can be selected as the optimal conditions.

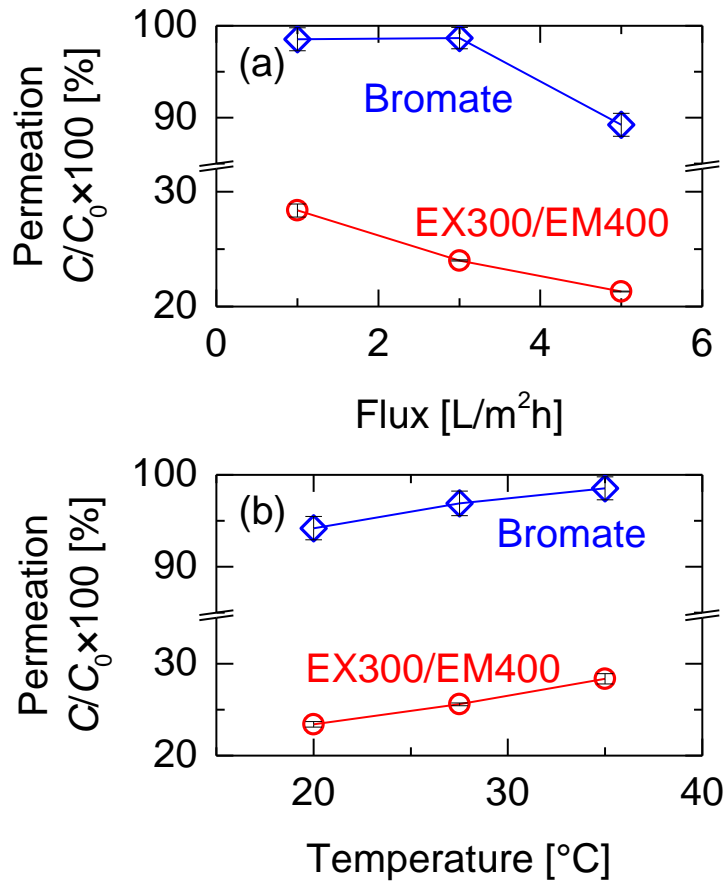


Fig. 6.2 Effects of (a) permeate flux and (b) feed temperature of the NF pre-treatment system on the permeation of bromate ions and the interfering substances in the MBR-treated wastewater represented by the fluorescence intensities (EX300/EM400). The standard permeate flux and feed temperature were 1 L/m² h and 35 °C, respectively. Bromate ion concentrations were adjusted to 12 µg/L.

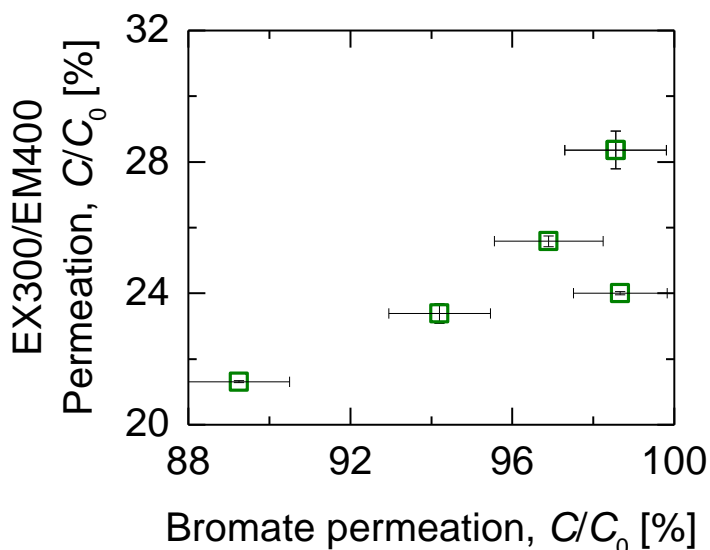
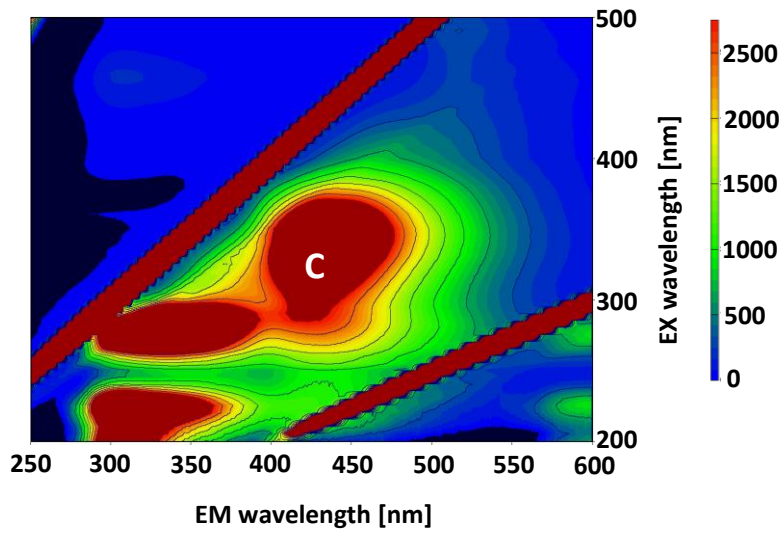


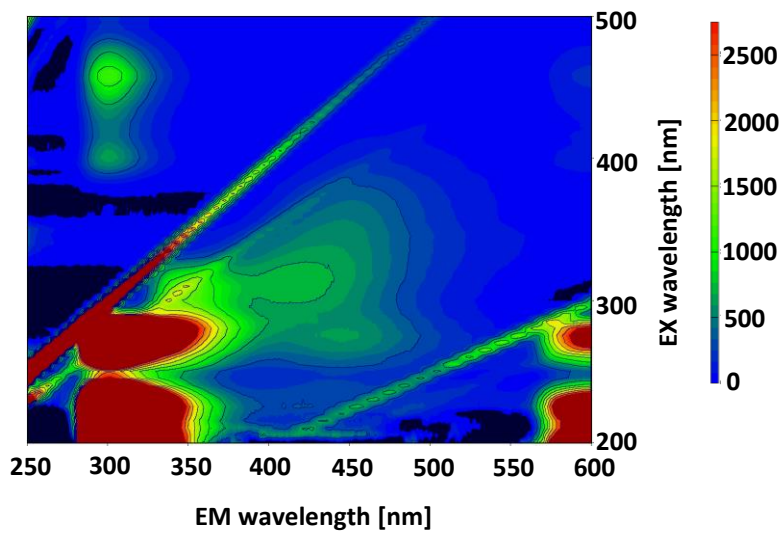
Fig. 6.3 The relationship between bromate ion permeation and EX300/EM400 permeation. The standard permeate flux and feed temperature were 1 L/m²h and 35 °C, respectively. Bromate ion concentrations in the MBR-treated effluent were adjusted at 12 µg/L, and analyzed using LC-MS/MS.

Bromate ion concentrations in the primary wastewater treatment effluent were also analyzed to assess the versatility of the NF pre-treatment system and identify its optimal treatment conditions (i.e., permeate flux of 1.0 L/m² h and feed temperature of 35 °C). Results showed that the permeation of bromate ions and interfering substances was 100% and 28%, respectively, during the NF pre-treatment, which was comparable to that of the MBR-treated wastewater. The online bromate ion analyzer did not show instrumental errors, despite high concentrations of interfering substances in the primary wastewater effluent. The intensity of humic acid-like fluorophores was substantially reduced using the NF pre-treatment system (**Fig. 6.4**). For a primary wastewater treatment effluent sample with bromate ion concentrations of 0.0 or 5.0 µg/L, determined using LC-MS/MS, the online analyzer coupled with the optimized NF pre-treatment system provided similar bromate ion concentrations (0.3 and 4.3 µg/L). Therefore, a permeate flux of 1 L/m² h and a feed

temperature of 35 °C were selected as the optimal conditions in this study because removing approximately 70 % of the interfering substances was adequate to eliminate instrumental errors.



(a) Feed



(b) Permeate

Fig. 6.4 Excitation and emission spectra of primary wastewater effluent: (a) before and (b) after NF pre-treatment. The data was attained during NF pre-treatment at a feed temperature of 35 °C and a permeate flux of 1 L/m²h.

6.3. Validations in the online analysis results

The efficiency of the online analyzer coupled with the optimized NF pre-treatment system was successfully demonstrated by monitoring MBR-treated wastewater, containing variable concentrations of bromate ions, over a course of three days (16 analyses/d) (**Fig. 6.5a**). During the experimental period, small variations were observed in bromate ion concentrations determined by using the online analyzer. For example, when an MBR-treated wastewater sample, containing a low target concentration of 3.0 $\mu\text{g/L}$, was analyzed from 0.2 d to 0.7 d, a variation of $3.1 \pm 0.5 \mu\text{g/L}$ was observed. Similar variations were observed at three different target concentrations (6.0, 9.0, and 12.0 $\mu\text{g/L}$). The accuracy of the online analytical data was determined by analyzing bromate ion concentrations in the split samples using LC–MS/MS. A strong linear correlation ($R^2 = 0.95$) was observed between bromate ion concentrations of 0 and 12 $\mu\text{g/L}$ (**Fig. 6.5**). Moreover, stable permeation rates for bromate ions ($94\% \pm 7\%$) (**Fig. 6.6**) and the interfering substances (approximately 20%) (**Fig. 6.7**) were observed. Based on the efficiency and accuracy of the online analyzer, the online-determined bromate ion concentration can be used to continuously monitor changes in bromate ion concentrations in treated wastewaters.

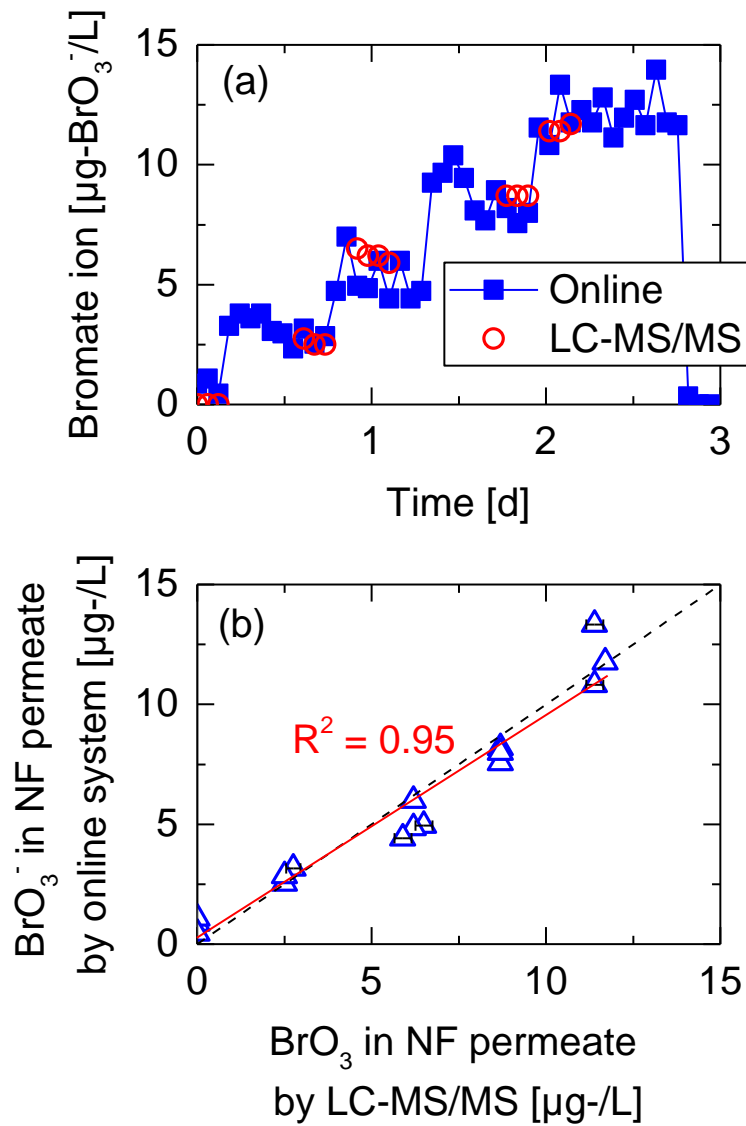


Fig. 6.5 (a) Bromate ion concentrations determined using liquid chromatography coupled with tandem mass spectrometry (LC-MS/MS) and the online bromate ion analyzer coupled with the NF pretreatment system (feed temperature: 35 °C; permeate flux: 1 L/m² h; transmembrane pressure: 30 kPa) and (b) correlation of the bromate ion concentrations analyzed using the two methods.

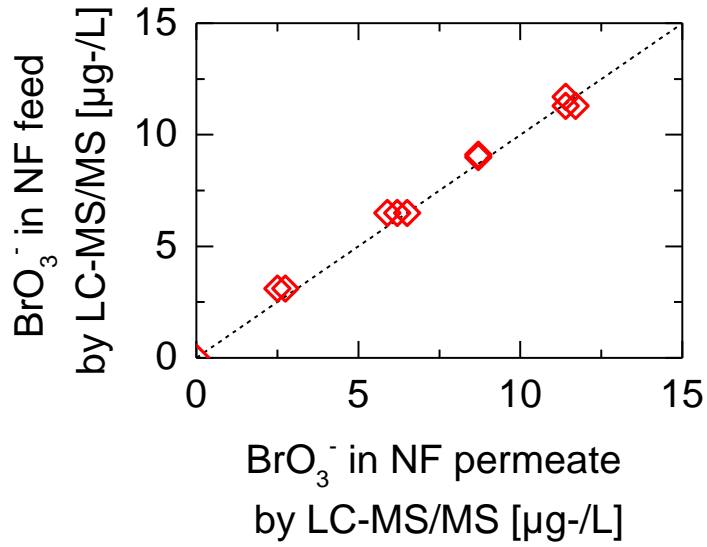


Fig. 6.6 Bromate concentrations before and after the NF pre-treatment system over a course of three days.

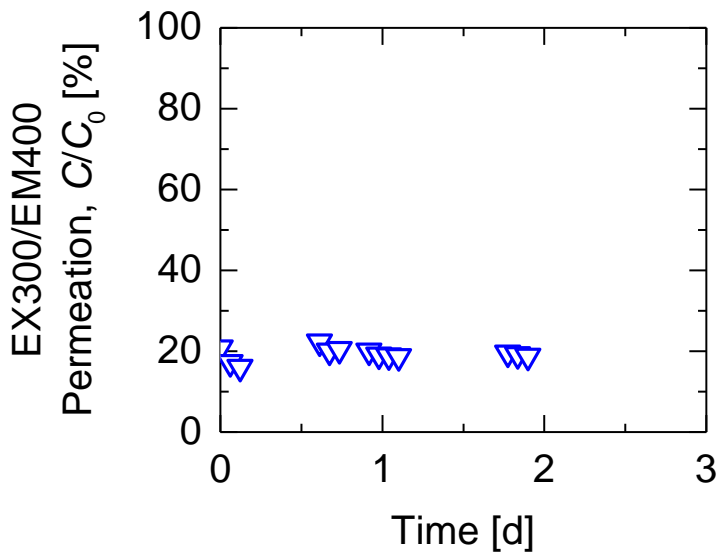


Fig. 6.7 Permeation of interfering substances represented by fluorescence intensity (EX300/EM400) over a course of three days.

However, further investigations are warranted to determine the potential of the NF pre-treatment system to estimate the quality parameters of different types of wastewater. For example, a 20%–30% decrease in the level of interfering substances may not be sufficient for

wastewater samples containing high concentrations of the interfering substances. Therefore, altering the permeation of bromate ions using the NF membrane (such as, a higher permeate flux leading to an increased removal of both bromate ions and interfering substances) may be necessary. Additionally, the minimal interference in the online bromate ion analyzer can be ensured by identifying NF membranes that can be used to remove humic acid-like substances without affecting the permeation of bromate ions. Another concern is the long-term stability of the NF pre-treatment system. The permeate flux in this study (1 L/m² h) was much lower than those used in representative NF treatment systems (20–40 L/m² h), inducing less membrane fouling. In addition, the transmembrane pressure of the NF pre-treatment system remained constant over three days, suggesting that membrane fouling was negligible.

6.4. Implications for on-site use

This study demonstrated the potential utility of an online bromate ion analyzer in combination with an NF pre-treatment system for detecting high bromate ion concentrations in treated wastewater. High bromate ion concentrations after ozonation can result from: (a) ozone generator or ozone-dosing control system failures (e.g., high ozone doses), (b) unpredictable increases in bromide ion concentrations in untreated wastewater, and (c) unpredictable formation of bromate ions, resulting from changes in the water quality of the ozonation influent, such as spikes in dissolved organic matter concentrations. Therefore, monitoring bromate ion concentrations immediately after ozonation will allow plant operators to implement countermeasures, such as ozone dose reductions. It is important to note that polymeric NF membranes and many components of the online bromate ion analyzer are not ozone-resistant. Therefore, residual ozone needs to be quenched by adding reducing agents (e.g., sodium thiosulfate) before it is measured by the online bromate ion analyzer.

Chapter 7 Conclusions

First, the peaks of 2-MIB concentrations and of *Pseudanabaena* sp. counts occurred at the same time in the studied lake, indicating that *Pseudanabaena* sp. can be a key indicator of odor occurrence. Diatoms and green algae exhibited high fluorescence intensity, whereas cyanobacteria including *Pseudanabaena* sp. had weak fluorescence intensity. This difference enabled the automatic distinction between diatoms/green algae and cyanobacteria including *Pseudanabaena* sp. The dimensions (i.e., length and width) of *Pseudanabaena* sp. in fluorescence observation mode were unique among other cyanobacteria, which enabled the automatic detection of *Pseudanabaena* sp. counts based on the dimensions and fluorescence intensity of algae. A high correlation between manually and automatically counted *Pseudanabaena* sp. was observed in lake water samples. Despite an inherent tendency to overestimate *Pseudanabaena* sp. counts, the developed auto-counting method was demonstrated to be a facile technique for counting *Pseudanabaena* sp. in lake waters. The developed technique therefore has important applications for the early detection and mitigation of odor in drinking water treatment plants.

Secondly, the stable attenuation of background interfering substances (humic acids) without any replacement parts was successfully achieved throughout the 19-d test with the pre-treatment system combining dialysis and anion exchange resins for dialysate regeneration. This allowed real-time counting of bacterial concentrations in the sand filter effluent without any dilution. Online bacterial counting of the sand filter effluent provided a profile of bacterial counts before and after backwashing and different concentration peaks were identified. Real-time bacteriological counter coupled with the pre-treatment system is one of the few tools for tracking the irregular variations in bacterial concentrations in water. Online-monitored bacterial counts and total bacterial counts determined by fluorescence microscopy were highly correlated. Therefore the real-time microbiological counter can provide an early

warning of filter malfunctions or potential contaminations in the sand filter effluent. This will allow plant operators to diagnose the overall system and provide countermeasures.

The last study demonstrated the potential of the NF pre-treatment system coupled with an online analyzer for monitoring bromate ion concentrations in MBR-treated wastewater samples. In contrast with the conventional table-top analytical methods used, such as LC-MS/MS, the online analyzer provides a continuous profile of the bromate ions concentrations during water recycling. Although the accuracy of the online analyzer may be lower than that of the conventional table-top analytical methods, the online-monitored data can be utilized as an indicator of high bromate ion concentrations exceeding the guideline-prescribed value (10 $\mu\text{g/L}$). The detection of high bromate ion concentrations can serve as a cautionary measure and may help improve the safety of potable water.

Overall, regular monitoring is critical to ensure compliance. The implementation of online sensors in drinking water treatment plants can enhance the quality and the safety of drinking water.

Chapter 8 Future research

Most studies on automatic algae counting in Japan and overseas aim to determine the total concentrations of cyanobacteria to analyze the occurrence of harmful algal bloom in lakes. However, the total cyanobacteria concentration does not necessarily act as odor indicator because odorous chemicals (2-MIB or geosmin) at concentrations higher than their regulated values (e.g., 10 ng/L) can be identified even when minor population of odor-producing cyanobacteria is present (e.g., <1%). This highlights the importance of individually counting odor-producing algae rather than bulk counting of the cyanobacteria. Future research is needed to monitor other odor producing algae. Then a flow cell and a pump could be added to the microscope to develop an online monitoring system. Moreover, the online algae counter developed could be used in combination with the online bacteria counter with the improved dialysis pretreatment. Together, they could create a breakthrough in ensuring the reliability of drinking water quality and safety.

About online bromate analysis using an NF membrane-based pretreatment system, long-term operation over several months may gradually promote membrane fouling, affecting the permeation of bromate ions and interfering substances. To ensure that the NF pre-treatment is continuous, stable, and efficient, membranes must be periodically replaced or membrane foulants must be removed by chemical cleaning. Therefore, on-site, long-term monitoring is warranted to assess the long-term viability of the NF pre-treatment system.

References

- Ahmad, R., Amirtharajah, A., Al-Shawwa, A. and Huck, P.M. (1998) Effects of backwashing on biological filters. *J. AWWA* 90(12), 62-73.
- Bacaro, F., Dickenson, E., Trenholm, R.A. and Gerrity, D. (2019) N-Nitrosodimethylamine (NDMA) formation and mitigation in potable reuse treatment trains employing ozone and biofiltration. *Environ. Sci.: Water Res. Technol.* 5(4), 713-725.
- Bertone, E., Burford, M.A. and Hamilton, D.P. (2018) Fluorescence probes for real-time remote cyanobacteria monitoring: A review of challenges and opportunities. *Water Research* 141, 152-162.
- Bertone, E., Chuang, A., Burford, M.A. and Hamilton, D.P. (2019) In-situ fluorescence monitoring of cyanobacteria: Laboratory-based quantification of species-specific measurement accuracy. *Harmful Algae* 87, 101625.
- Besmer, M.D., Sigrist, J.A., Props, R., Buyschaert, B., Mao, G., Boon, N. and Hammes, F. (2017) Laboratory-Scale Simulation and Real-Time Tracking of a Microbial Contamination Event and Subsequent Shock-Chlorination in Drinking Water. *Frontiers in microbiology* 8, 1900-1900.
- Besmer, M.D., Weissbrodt, D.G., Kratochvil, B.E., Sigrist, J.A., Weyland, M.S. and Hammes, F. (2014) The feasibility of automated online flow cytometry for in-situ monitoring of microbial dynamics in aquatic ecosystems. *Frontiers in Microbiology* 5, 265.
- Butler, R., Lytton, L., Godley, A.R., Tothill, I.E. and Cartmell, E. (2005) Bromate analysis in groundwater and wastewater samples. *J. Environ. Monit.* 7(10), 999-1006.
- Buyschaert, B., Vermijs, L., Naka, A., Boon, N. and De Gussemé, B. (2018) Online flow cytometric monitoring of microbial water quality in a full-scale water treatment plant. *npj Clean Water* 1(1), 16.
- Carstea, E.M., Bridgeman, J., Baker, A. and Reynolds, D.M. (2016) Fluorescence spectroscopy for wastewater monitoring: A review. *Water Res.* 95, 205-219.
- Cescon, A. and Jiang, J.-Q. (2020) Filtration Process and Alternative Filter Media Material in Water Treatment. *Water* 12(12), 3377.
- Chan, S., Pullerits, K., Keucken, A., Persson, K.M., Paul, C.J. and Rådström, P. (2019) Bacterial release from pipe biofilm in a full-scale drinking water distribution system. *npj Biofilms and Microbiomes* 5(1), 9.

- Chang, D.-W., Hobson, P., Burch, M. and Lin, T.-F. (2012) Measurement of cyanobacteria using in-vivo fluoroscopy – Effect of cyanobacterial species, pigments, and colonies. *Water Research* 46(16), 5037-5048.
- Chen, W., Westerhoff, P., Leenheer, J.A. and Booksh, K. (2003) Fluorescence excitation–emission matrix regional integration to quantify spectra for dissolved organic matter. *Environ. Sci. Technol.* 37(24), 5701-5710.
- Coltelli, P., Barsanti, L., Evangelista, V., Frassanito, A.M. and Gualtieri, P. (2014) Water monitoring: automated and real time identification and classification of algae using digital microscopy. *Environ Sci Process Impacts* 16(11), 2656-2665.
- Colton, J.F., Hillis, P. and Fitzpatrick, C.S.B. (1996) Filter backwash and start-up strategies for enhanced particulate removal. *Water Res.* 30(10), 2502-2507.
- CSWRCB (2016) Investigation on the feasibility of developing uniform water recycling criteria for direct potable reuse, Sacramento, CA.
- Deglint, J.L., Jin, C., Chao, A. and Wong, A. (2019) The Feasibility of Automated Identification of Six Algae Types Using Feed-Forward Neural Networks and Fluorescence-Based Spectral-Morphological Features. *IEEE Access* 7, 7041-7053.
- Dow, C., Ahmad, S., Stave, K. and Gerrity, D. (2019) Evaluating the sustainability of indirect potable reuse and direct potable reuse: a southern Nevada case study. *AWWA Water Science* 1(4), e1153.
- El-Chakhtoura, J., Prest, E., Saikaly, P., van Loosdrecht, M., Hammes, F. and Vrouwenvelder, H. (2015) Dynamics of bacterial communities before and after distribution in a full-scale drinking water network. *Water Res.* 74, 180-190.
- Embleton, K., Gibson, C.E. and Heaney, S. (2003) Automated counting of phytoplankton by pattern recognition: a comparison with a manual counting method. *Journal of Plankton Research* 25, 669-681.
- Ernst, B., Naser, S., O'Brien, E., Hoeger, S.J. and Dietrich, D.R. (2006) Determination of the filamentous cyanobacteria *Planktothrix rubescens* in environmental water samples using an image processing system. *Harmful Algae* 5(3), 281-289.
- Faruqi, A., Henderson, M., Henderson, R.K., Stuetz, R., Gladman, B., McDowall, B. and Zamyadi, A. (2018) Removal of algal taste and odour compounds by granular and biological activated carbon in full-scale water treatment plants. *Water Supply* 18(5), 1531-1544.
- Fujioka, T. and Boivin, S. (2020a) Assessing bacterial infiltration through reverse osmosis membrane. *Environmental Technology & Innovation* 19, 100818.

- Fujioka, T. and Boivin, S. (2020b) Dialysis as a new pre-treatment technique for online bacterial counting. *Sci. Total Environ.* 714, 136768.
- Fujioka, T., Hoang, A.T., Aizawa, H., Ashiba, H., Fujimaki, M. and Leddy, M. (2018) Real-Time Online Monitoring for Assessing Removal of Bacteria by Reverse Osmosis. *Environ. Sci. Technol. Letters* 5(6), 389-393.
- Fujioka, T., Khan, S.J., McDonald, J.A. and Nghiem, L.D. (2015) Rejection of trace organic chemicals by a nanofiltration membrane: the role of molecular properties and effects of caustic cleaning. *Environ. Sci.: Water Res. Technol.* 1(6), 846-854.
- Fujioka, T., Makabe, R., Mori, N., Snyder, S.A. and Leddy, M. (2019a) Assessment of online bacterial particle counts for monitoring the performance of reverse osmosis membrane process in potable reuse. *Sci. Total Environ.* 667, 540-544.
- Fujioka, T., Ngo, M.T.T., Makabe, R., Boivin, S. and Ikehata, K. (2021) Pretreatment of Surface Waters and Wastewater by a Hemodiafilter for Online Bacterial Counting. *ACS ES&T Water* 1(1), 101-107.
- Fujioka, T., Ueyama, T., Mingliang, F. and Leddy, M. (2019b) Online assessment of sand filter performance for bacterial removal in a full-scale drinking water treatment plant. *Chemosphere* 229, 509-514.
- Graham, M.D., Cook, J., Graydon, J., Kinniburgh, D., Nelson, H., Piliéci, S. and Vinebrooke, R.D. (2018) High-resolution imaging particle analysis of freshwater cyanobacterial blooms. *Limnology and Oceanography: Methods* 16(10), 669-679.
- Gregor, J. and Maršálek, B. (2004) Freshwater phytoplankton quantification by chlorophyll a: a comparative study of in vitro, in vivo and in situ methods. *Water Research* 38(3), 517-522.
- Gunnarsdottir, M.J., Gardarsson, S.M., Figueras, M.J., Puigdomènech, C., Juárez, R., Saucedo, G., Arnedo, M.J., Santos, R., Monteiro, S., Avery, L., Pagaling, E., Allan, R., Abel, C., Eglitis, J., Hambsch, B., Hügler, M., Rajkovic, A., Smigic, N., Udovicki, B., Albrechtsen, H.-J., López-Avilés, A. and Hunter, P. (2020) Water safety plan enhancements with improved drinking water quality detection techniques. *Sci. Total Environ.* 698, 134185.
- Hammes, F., Broger, T., Weilenmann, H.-U., Vital, M., Helbing, J., Bosshart, U., Huber, P., Peter Odermatt, R. and Sonnleitner, B. (2012) Development and laboratory-scale testing of a fully automated online flow cytometer for drinking water analysis. *Cytometry Part A* 81A(6), 508-516.

- Hense, B.A., Gais, P., Jütting, U., Scherb, H. and Rodenacker, K. (2008) Use of fluorescence information for automated phytoplankton investigation by image analysis. *Journal of Plankton Research* 30(5), 587-606.
- Højris, B., Kornholt, S.N., Christensen, S.C.B., Albrechtsen, H.J. and Olesen, L.S. (2018) Detection of drinking water contamination by an optical real-time bacteria sensor. *H2Open Journal* 1(2), 160-168.
- Hooper, J., Funk, D., Bell, K., Noibi, M., Vickstrom, K., Schulz, C., Machek, E. and Huang, C.-H. (2020) Pilot testing of direct and indirect potable water reuse using multi-stage ozone-biofiltration without reverse osmosis. *Water Res.* 169, 115178.
- Huber, S.A., Balz, A., Abert, M. and Pronk, W. (2011) Characterisation of aquatic humic and non-humic matter with size-exclusion chromatography – organic carbon detection – organic nitrogen detection (LC-OCD-OND). *Water Res.* 45(2), 879-885.
- Ives, K.J. (1970) Rapid filtration. *Water Res.* 4(3), 201-223.
- Izaguirre, G. and Taylor, W. (2004) A guide to geosmin-and MIB-producing cyanobacteria in the United States. *Water Science and Technology* 49(9), 19-24.
- Jahan, B.N., Li, L. and Pagilla, K.R. (2021) Fate and reduction of bromate formed in advanced water treatment ozonation systems: A critical review. *Chemosphere* 266, 128964.
- Kajino, M. and Sakamoto, K. (1995) The relationship between musty-odor-causing organisms and water quality in Lake Biwa. *Water Science and Technology* 31(11), 153-158.
- Kim, K., Yoon, Y., Cho, H. and Hwang, S.-J. (2020) Molecular Probes to Evaluate the Synthesis and Production Potential of an Odorous Compound (2-methylisoborneol) in Cyanobacteria. *International Journal of Environmental Research and Public Health* 17(6), 1933.
- Kim, Y., Lee, Y., Gee, C.S. and Choi, E. (1997) Treatment of taste and odor causing substances in drinking water. *Water Sci. Technol.* 35(8), 29-36.
- Lee, J. and Deininger, R.A. (1999) A RAPID METHOD FOR DETECTING BACTERIA IN DRINKING WATER. *Journal of Rapid Methods & Automation in Microbiology* 7(2), 135-145.
- Lee, J.E., Youn, S.-J., Byeon, M. and Yu, S.-J. (2020) Occurrence of cyanobacteria, actinomycetes, and geosmin in drinking water reservoir in Korea: a case study from an algal bloom in 2012. *Water Supply* 20(5), 1862-1870.

- Li, Q., Gu, P., Zhang, H., Luo, X., Zhang, J. and Zheng, Z. (2020) Response of submerged macrophytes and leaf biofilms to the decline phase of *Microcystis aeruginosa*: Antioxidant response, ultrastructure, microbial properties, and potential mechanism. *Science of The Total Environment* 699, 134325.
- Lin, D., Liang, H. and Li, G. (2020) Factors affecting the removal of bromate and bromide in water by nanofiltration. *Environ. Sci. Pollut. R.* 27(20), 24639-24649.
- Liu, G., Zhang, Y., van der Mark, E., Magic-Knezev, A., Pinto, A., van den Bogert, B., Liu, W., van der Meer, W. and Medema, G. (2018) Assessing the origin of bacteria in tap water and distribution system in an unchlorinated drinking water system by SourceTracker using microbial community fingerprints. *Water Res.* 138, 86-96.
- Matsui, Y., Aizawa, T., Suzuki, M. and Kawase, Y. (2007) Removal of geosmin and algae by ceramic membrane filtration with super-powdered activated carbon adsorption pretreatment. *Water Supply* 7(5-6), 43-51.
- McGoverin, C., Robertson, J., Jonmohamadi, Y., Swift, S. and Vanholsbeeck, F. (2020) Species Dependence of SYTO 9 Staining of Bacteria. *Frontiers in Microbiology* 11(2149).
- Millie, D., Pigg, R., Fahnenstiel, G. and Carrick, H. (2010), pp. 93-122.
- Nam, S.-N. and Amy, G. (2008) Differentiation of wastewater effluent organic matter (EfOM) from natural organic matter (NOM) using multiple analytical techniques. *Water Sci. Technol.* 57(7), 1009-1015.
- Nescerecka, A., Juhna, T. and Hammes, F. (2018) Identifying the underlying causes of biological instability in a full-scale drinking water supply system. *Water Res.* 135, 11-21.
- Nghiem, L.D., Schäfer, A.I. and Elimelech, M. (2005) Pharmaceutical retention mechanisms by nanofiltration membranes. *Environ. Sci. Technol.* 39(19), 7698-7705.
- Niiyama, Y., Tuji, A., Takemoto, K. and Ichise, S. (2016a) *Pseudanabaena foetida* sp. nov. and *P. subfoetida* sp. nov. (Cyanophyta/ Cyanobacteria) producing 2-methylisoborneol from Japan. *Fottea* 16.
- Niiyama, Y., Tuji, A., Takemoto, K. and Ichise, S. (2016b) *Pseudanabaena foetida* sp. nov. and *P. subfoetida* sp. nov. (Cyanophyta/ Cyanobacteria) producing 2-methylisoborneol from Japan. *Fottea* 16(1), 1-11.
- Noibi, M., Hooper, J., Bell, K. and Funk, D. (2020) Direct potable reuse using full advanced treatment versus ozone biofiltration: A cost comparison. *AWWA Water Science* 2(6), e1210.

- Ohtomo, T., Yatabe, R., Tanaka, Y., Kato, J., Igarashi, S. and Tower, S.T. (2009) Fluorescence detection-FIA for ppb levels of bromate with trifluoperazine. *Journal of flow injection analysis* 26, 127-131.
- Oikawa, E. and Ishibashi, Y. (2004) Species specificity of musty odor producing *Phormidium tenue* in Lake Kamafusa. *Water science and technology : a journal of the International Association on Water Pollution Research* 49, 41-46.
- Olesen, L.S., Højris, B. and Folia, N.B. (2018) *Microbiological Sensors for the Drinking Water Industry*. Skovhus, T.L. and Højris, B. (eds), IWA Publishing.
- Park, J.W., Kim, H.-C., Meyer, A.S., Kim, S. and Maeng, S.K. (2016) Influences of NOM composition and bacteriological characteristics on biological stability in a full-scale drinking water treatment plant. *Chemosphere* 160, 189-198.
- Park, M., Anumol, T. and Snyder, S.A. (2015) Modeling approaches to predict removal of trace organic compounds by ozone oxidation in potable reuse applications. *Environ. Sci.: Water Res. Technol.* 1(5), 699-708.
- Pecson, B.M., Triolo, S.C., Olivieri, S., Chen, E.C., Pisarenko, A.N., Yang, C.-C., Olivieri, A., Haas, C.N., Trussell, R.S. and Trussell, R.R. (2017) Reliability of pathogen control in direct potable reuse: Performance evaluation and QMRA of a full-scale 1 MGD advanced treatment train. *Water Res.* 122, 258-268.
- Pepper, I.L. and Snyder, S.A. (2016) *Monitoring for reliability and process control of potable reuse applications*, Water Environment & Reuse Foundation and IWA Publishing, Alexandria, VA.
- Phe, M.-H., Dossot, M., Guilloteau, H. and Block, J.-C. (2005) Nucleic acid fluorochromes and flow cytometry prove useful in assessing the effect of chlorination on drinking water bacteria. *Water Res.* 39(15), 3618-3628.
- Potgieter, S., Pinto, A., Sigudu, M., du Preez, H., Ncube, E. and Venter, S. (2018) Long-term spatial and temporal microbial community dynamics in a large-scale drinking water distribution system with multiple disinfectant regimes. *Water Res.* 139, 406-419.
- Ramseier, M.K., von Gunten, U., Freihofer, P. and Hammes, F. (2011) Kinetics of membrane damage to high (HNA) and low (LNA) nucleic acid bacterial clusters in drinking water by ozone, chlorine, chlorine dioxide, monochloramine, ferrate(VI), and permanganate. *Water Res.* 45(3), 1490-1500.
- Rong, C., Liu, D., Li, Y., Yang, K., Han, X., Yu, J., Pan, B., Zhang, J. and Yang, M. (2018) Source water odor in one reservoir in hot and humid areas of southern China:

- occurrence, diagnosis and possible mitigation measures. *Environmental Sciences Europe* 30(1), 45.
- Rouso, B.Z., Bertone, E., Stewart, R. and Hamilton, D.P. (2020) A systematic literature review of forecasting and predictive models for cyanobacteria blooms in freshwater lakes. *Water Research* 182, 115959.
- Ruffino, B., Korshin, G.V. and Zanetti, M. (2020) Use of spectroscopic indicators for the monitoring of bromate generation in ozonated wastewater containing variable concentrations of bromide. *Water Res.* 182, 116009.
- Sakai, K. (1994) Determination of pore size and pore size distribution: 2. Dialysis membranes. *J. Membr. Sci.* 96(1), 91-130.
- Sawyer, L.K. and Hermanowicz, S.W. (1998) Detachment of biofilm bacteria due to variations in nutrient supply. *Water Sci. Technol.* 37(4-5), 211-214.
- Schulze, K., Tillich, U.M., Dandekar, T. and Frohme, M. (2013) PlanktoVision - an automated analysis system for the identification of phytoplankton. *BMC Bioinformatics* 14(1), 115.
- Sharma, R.R., Agrawal, R. and Chellam, S. (2003) Temperature effects on sieving characteristics of thin-film composite nanofiltration membranes: pore size distributions and transport parameters. *J. Membr. Sci.* 223(1-2), 69-87.
- Sherchan, S.P., Gerba, C.P. and Pepper, I.L. (2013) Evaluation of Real-Time Water Quality Sensors for the Detection of Intentional Bacterial Spore Contamination of Potable Water. *Journal of Biosensors & Bioelectronics* 4(4), 1-5.
- Shi, J.L., Plata, S.L., Kleimans, M., Childress, A.E. and McCurry, D.L. (2021) Formation and Fate of Nitromethane in Ozone-Based Water Reuse Processes. *Environ. Sci. Technol.* 55(9), 6281-6289.
- Shizuka, K., Ikenaga, M., Murase, J., Nakayama, N., Matsuya, N., Kakino, W., Taruya, H. and Maie, N. (2020) Diversity of 2-MIB-Producing cyanobacteria in Lake Ogawara: microscopic and molecular ecological approaches. *Aquaculture Science* 68(1), 9-23.
- Skovhus, T.L. and Højris, B. (2018) *Microbiological Sensors for the Drinking Water Industry*, IWA Publishing.
- Snyder, S.A., Vanderford, B.J. and Rexing, D.J. (2005) Trace Analysis of Bromate, Chlorate, Iodate, and Perchlorate in Natural and Bottled Waters. *Environ. Sci. Technol.* 39(12), 4586-4593.

- Soyer, E., Akgiray, Ö., Eldem, N.Ö. and Saatçı, A.M. (2013) On the Use of Crushed Recycled Glass Instead of Silica Sand in Dual-Media Filters. *CLEAN – Soil, Air, Water* 41(4), 325-332.
- Srinivasan, R. and Sorial, G. (2011) Treatment of taste and odor causing compounds 2-methyl isoborneol and geosmin in drinking water: A critical review. *Journal of environmental sciences (China)* 23, 1-13.
- Stadler, P., Blöschl, G., Vogl, W., Koschelnic, J., Epp, M., Lackner, M., Oismüller, M., Kumpan, M., Nemeth, L., Strauss, P., Sommer, R., Ryzinska-Paier, G., Farnleitner, A.H. and Zessner, M. (2016) Real-time monitoring of beta-d-glucuronidase activity in sediment laden streams: A comparison of prototypes. *Water Res.* 101, 252-261.
- Stiefel, P., Schmidt-Emrich, S., Maniura-Weber, K. and Ren, Q. (2015) Critical aspects of using bacterial cell viability assays with the fluorophores SYTO9 and propidium iodide. *BMC Microbiol.* 15(1), 36.
- Sugiura, N., Iwami, N., Inamori, Y., Nishimura, O. and Sudo, R. (1998) Significance of attached cyanobacteria relevant to the occurrence of musty odor in Lake Kasumigaura. *Water Research* 32(12), 3549-3554.
- Takahashi, T. (2018) Applicability of Automated Cell Counter with a Chlorophyll Detector in Routine Management of Microalgae. *Scientific Reports* 8(1), 4967.
- Takemoto, K., Yoshimura, M., Yamamoto, A., Ichise, S., Namba, H. and Kihara, H. (2016) Imaging of musty-odor producing filamentous cyanobacteria by various microscopies. *AIP Conference Proceedings* 1696(1), 020024.
- Tchobanoglous, G., Cotruvo, J., Crook, J., McDonald, E., Olivieri, A., Salveson, A. and Trussell, R.S. (2015) Framework for direct potable reuse, WateReuse Association, American Water Works Association, Water Environment Federation, National Water Research Institute, Alexandria, VA.
- Tsai, Y.-P. (2005) Impact of flow velocity on the dynamic behaviour of biofilm bacteria. *Biofouling* 21(5-6), 267-277.
- Tsuru, T., Ogawa, K., Kanazashi, M. and Yoshioka, T. (2010) Permeation characteristics of electrolytes and neutral solutes through titania nanofiltration membranes at high temperatures. *Langmuir* 26(13), 10897-10905.
- Tuji, A. and Niiyama, Y. (2018) Two new *Pseudanabaena* (Cyanobacteria, Synechococcales) species from Japan, *Pseudanabaena cinerea* and *Pseudanabaena yagii*, which produce 2-methylisoborneol. *Phycol. Res.* 66(4), 291-299.

- Van Nevel, S., Koetzsch, S., Proctor, C.R., Besmer, M.D., Prest, E.I., Vrouwenvelder, J.S., Knezev, A., Boon, N. and Hammes, F. (2017) Flow cytometric bacterial cell counts challenge conventional heterotrophic plate counts for routine microbiological drinking water monitoring. *Water Res.* 113, 191-206.
- Vatankhah, H., Szczuka, A., Mitch, W.A., Almaraz, N., Brannum, J. and Bellona, C. (2019) Evaluation of Enhanced Ozone–Biologically Active Filtration Treatment for the Removal of 1,4-Dioxane and Disinfection Byproduct Precursors from Wastewater Effluent. *Environ. Sci. Technol.* 53(5), 2720-2730.
- Virto, R., Mañas, P., Álvarez, I., Condon, S. and Raso, J. (2005) Membrane Damage and Microbial Inactivation by Chlorine in the Absence and Presence of a Chlorine-Demanding Substrate. *Appl. Environ. Microbiol.* 71(9), 5022-5028.
- Watson, S.B. (2004) Aquatic taste and odor: a primary signal of drinking-water integrity. *Journal of Toxicology and Environmental Health, Part A* 67(20-22), 1779-1795.
- Watson, S.B., Monis, P., Baker, P. and Giglio, S. (2016) Biochemistry and genetics of taste- and odor-producing cyanobacteria. *Harmful Algae* 54, 112-127.
- Wei, B., Sugiura, N. and Maekawa, T. (2001) Use of artificial neural network in the prediction of algal blooms. *Water Research* 35(8), 2022-2028.
- Wei, J., Gao, B., Yue, Q., Wang, Y., Li, W. and Zhu, X. (2009) Comparison of coagulation behavior and floc structure characteristic of different polyferric-cationic polymer dual-coagulants in humic acid solution. *Water Res.* 43(3), 724-732.
- Welfare, M.o.H.L.a. (2015) Drinking Water Quality Standard, Japan.
- WHO (2011) Guidelines for drinking-water quality 4th edition.
- Wijmans, J.G. and Baker, R.W. (1995) The solution-diffusion model: a review. *J. Membr. Sci.* 107(1–2), 1-21.
- Winter, J.G., DeSellas, A.M., Fletcher, R., Heintsch, L., Morley, A., Nakamoto, L. and Utsumi, K. (2011) Algal blooms in Ontario, Canada: increases in reports since 1994. *Lake and Reservoir Management* 27(2), 107-114.
- Wu, M., Yu, W., Qu, J. and Gregory, J. (2019) The variation of flocs activity during floc breakage and aging, adsorbing phosphate, humic acid and clay particles. *Water Res.* 155, 131-141.
- Yagi, M., Kajino, M., Matsuo, U., Ashitani, K., Kita, T. and Nakamura, T. (1983) Odor Problems in Lake Biwa. *Water Science and Technology* 15(6-7), 311-321.
- Yoon, S.-H. (2019) Potential and limitation of fluorescence-based membrane integrity monitoring (FMIM) for reverse osmosis membranes. *Water Res.* 154, 287-297.

Zhang, T., Zheng, L., Li, L. and Song, L. (2016) 2-Methylisoborneol production characteristics of *Pseudanabaena* sp. FACHB 1277 isolated from Xionghe Reservoir, China. *J. Appl. Phycol.* 28(6), 3353-3362.